

# A three-pillar approach to assessing climate impacts on low flows

G. Laaha<sup>1</sup>, J. Parajka<sup>2</sup>, A. Viglione<sup>2</sup>, D. Koffler<sup>1</sup>, K. Haslinger<sup>3</sup>, W. Schöner<sup>4</sup>, J. Zehetgruber<sup>1</sup> and G. Blöschl<sup>2</sup>

[1]{Institute of Applied Statistics and Computing, University of Natural Resources and Life Sciences (BOKU), Vienna, Austria}

[2]{Institute for Hydraulic and Water Resources Engineering, Vienna University of Technology, Vienna, Austria}

[3]{Climate Research Department, Central Institute for Meteorology and Geodynamics, Vienna, Austria}

[4]{Department of Geography and Regional Science, University of Graz, Graz, Austria}

Correspondence to: G. Laaha (gregor.laaha@boku.ac.at)

## Abstract

The objective of this paper is to present a framework for assessing climate impacts on future low flows that combines different sources of information, termed pillars. To illustrate the framework three pillars are chosen: (a) Extrapolation of observed low flow trends into the future; (b) Rainfall-runoff projections based on climate scenarios; (c) Extrapolation of changing stochastic rainfall characteristics into the future combined with rainfall-runoff modelling. Alternative pillars could be included in the overall framework. The three pillars are combined by expert judgement based on a synoptic view of data, model outputs and process reasoning. The consistency/inconsistency between the pillars is considered an indicator of the certainty/uncertainty of the projections. The viability of the framework is illustrated for four example catchments from Austria that represent typical climate conditions in Central Europe. In the Alpine region where winter low flows dominate, trend projections and climate scenarios yield consistently increasing low flows, although of different magnitudes. In the region north of the Alps, consistently small changes are projected by all methods. In the regions in the South and Southeast, more pronounced and mostly decreasing trends are projected but there is disagreement in the magnitudes of the projected changes. The process reasons for the consistencies/inconsistencies are discussed. For an Alpine region such as Austria the key to understanding low flows is whether they are controlled by freezing and snow melt processes, or by the summer moisture deficit associated with evaporation. It is argued that the three-pillar approach offers a systematic framework of combining different sources of information aiming at more robust projections than obtained from each pillar alone.

## 1 Introduction

Streamflow regimes are changing around the world due to multiple factors and low flows are often particularly affected. Direct human impacts, such as abstractions, and climate impacts are difficult to isolate (Blöschl and Montanari, 2010), yet understanding the causes of changes is essential for many water management tasks. Research into assessing low flow and drought changes falls into two groups (Sivapalan et al., 2003).

1 The first group infers catchment functioning from an interpretation of the observed streamflow  
2 response at the catchment scale. It includes statistical trend analyses of observed low flow  
3 characteristics, such as the annual minima, supported by analyses and interpretations of the  
4 process causes (e.g. Giuntoli et al. (2013) in France, Hannaford and Buys (2012) in the UK,  
5 Wilson et al. (2010) in the Nordic Countries, Lorenzo-Lacruz et al. (2012) on the Iberian  
6 peninsula, and Lins and Slack (1999) and Douglas et al. (2000) in the US). Most trend analyses  
7 are performed locally on a station-by-station basis and are therefore not fully conclusive at the  
8 larger scale of climate processes. Regional trend analyses are based on field significance  
9 statistics or block-bootstrapping procedures (e.g. Renard et al., 2008; Wilson et al., 2010) or,  
10 alternatively, a regional interpretation of trend patterns (e.g. Stahl et al., 2010). Most studies  
11 perform trend interpretations in a heuristic way without cross checking against alternative  
12 sources of information.

13 The second group involves a model cascade, where General Circulation Model (GCMs) outputs  
14 are fed into Regional Climate models (RCM), the outputs of which (usually precipitation and  
15 air temperature) are fed into hydrological models to project future streamflows. Low flow  
16 examples include De Wit et al. (2007) for the Meuse, Hurkmans et al. (2010) for the Rhine and  
17 Majone et al. (2012) for the Gállego river in Spain. National studies include Wong et al. (2011)  
18 in Norway, Prudhomme et al. (2012) in the UK, Chauveau et al. (2013) in France and Blöschl  
19 et al. (2011) in Austria. The hydrological models used in these studies are often not specifically  
20 parameterised for low flows which results in considerable uncertainties.

21 The two approaches have relative strengths and weaknesses (see Hall et al., 2014 for the flood  
22 case). The first approach makes fewer assumptions and is more directly based on observations  
23 but any extrapolation into the future is more speculative. Recent changes in air temperature  
24 have been quite consistent over time in many parts of the world. In the European Alps, for  
25 example, the increase in air temperature since 1980 has been about 0.5°C/decade with little  
26 variation between the decades (Böhm et al., 2001; Auer et al., 2007), and the expected trends  
27 are similar. If one assumes that air temperature is the main driver of low flow changes,  
28 persistence of low flow changes into the near future is therefore a reasonable assumption. Of  
29 course, such an extrapolation hinges on the realism of the assumptions and is likely only  
30 applicable to a limited time horizon. The second approach on the other hand is more process  
31 based, so has more potential for projections into the future, but the spatial resolution of the  
32 atmospheric models is rather coarse (e.g., 10 km for dynamically downscaled reclip:century  
33 simulations), so small-scale climate features, such as cloud formation and rainfall generation,  
34 cannot be resolved. As a consequence, air temperature projections tend to be more robust than  
35 precipitation projections, in particular in Alpine landscapes (Field and Intergovernmental Panel  
36 on Climate Change, 2012; Haslinger et al., 2013). There is value therefore in confronting such  
37 projections with results from other approaches.

38

## 39 **2 Three pillar approach**

40 In this paper we propose a framework that combines complementary pieces of information on  
41 low flows in order to enhance the reliability of the projections. The overall philosophy has been  
42 inspired by the concept of multi model climate projections where the projections from a group  
43 of models together are considered to be more robust than the individual projections, and the  
44 difference between the individual models represents an indicator of the uncertainty associated  
45 with the projections. Knutti et al. (2010, p. 2), for example, states: “Ensemble: A group of  
46 comparable model simulations. The ensemble can be used to gain a more accurate estimate of  
47 a model property through the provision of a larger sample size, e.g., of a climatological mean

1 of the frequency of some rare event. Variation of the results across the ensemble members gives  
2 an estimate of uncertainty.” While the climate models Knutti et al. (2010) are referring to are  
3 similar in their basic design and only differ in specific process representations, the notion of  
4 inferring predictive reliability from model consistency builds on the broader principle of  
5 consilience, which suggests that, if multiple sources of independent evidence are in agreement,  
6 the conclusion can be very strong even if the individual sources do not provide strong evidence  
7 on their own (Wilson, 1998). Combining different sources of information has a long tradition  
8 in various fields of hydrology such as flood estimation (Stedinger and Tasker, 1985; Gutknecht  
9 et al., 2006; Merz and Blöschl, 2008), low flow estimation, (Laaha and Blöschl, 2007) and,  
10 more generally, uncertainty estimation in ungauged basins (Gupta et al., 2013).

11 The combination can be based on formal methods such as Bayesian statistics (Viglione et al.,  
12 2013) or on a heuristic process reasoning based on expert judgement (Merz and Blöschl, 2008).  
13 The latter is able to account for a broader class of information sources but it is more subjective.  
14 In this paper, we chose a heuristic approach because of its flexibility but, as demonstrated by  
15 Viglione et al. (2013), this could be formalised.

16 We illustrate the framework by choosing three pillars or sources of information to assist in  
17 projecting low flows into the future. The first pillar consists of extrapolating observed low flow  
18 trends into the future. The second pillar consists of rainfall-runoff projections driven by GCM  
19 based climate scenarios. The third pillar extrapolates observed trends in stochastic rainfall and  
20 temperature characteristics into the future, combined with rainfall-runoff modelling.  
21 Alternative or additional pillars could be used, e.g., the “trading space for time” approach  
22 (Perdigão and Blöschl, 2014) where spatial gradients are transposed into temporal changes.

23 The data and assumptions of the three pillars differ, so one would also expect the error structures  
24 to be different which will have a number of benefits for the projections. Comparisons of  
25 observed and simulated low flow time series at the decadal time scale provide insight into the  
26 performance of the runoff models as well as the climate hindcasts which gives an indication of  
27 their performance for the future. The analysis and projection of the stochastic climate and low  
28 flow behaviour shed light on their co-behaviour, the sensitivity of low flows to changing climate  
29 variables and the role of noise over decadal time scales. Finally, the consistency of the  
30 projections by the different methods sheds light on the robustness of the overall projections.

31 We demonstrate the viability of the approach for four example regions in Austria and discuss  
32 the findings in the context of hydrological climate impact studies.

33

### 34 **3 Case study regions and data**

35 The four example regions are representative of the main climatological units in Austria.  
36 Although Austria is quite diverse, each of these regions is rather homogeneous in terms of  
37 climate and hydrological regime. Within each region, a typical catchment was selected guided  
38 by previous low flow and drought studies (Haslinger et al., 2014; Van Loon and Laaha, 2015).

39 The Hoalp region (for Hochalpen) is located in the Alps and exhibits a clear winter low flow  
40 regime where freeze and snow processes are important, so long-term trends are expected to be  
41 related to changing air temperatures. The region is represented by the Matreier Tauernhaus  
42 catchment at the Tauernbach (60 km<sup>2</sup> area, 1502 m.a.s.l. altitude). The Muhlv region (for  
43 Mühlviertel) is located north of the Alps and exhibits a dominant summer low flow regime as  
44 a result of summer precipitation and evaporation, so precipitation and air temperature will be  
45 important low flow controls. The region is represented by the Hartmannsdorf catchment at the  
46 Steinerne Mühl (138 km<sup>2</sup> area, 500 m altitude). The Gurk region (for Gurktal) is located south

1 of the Alps and also exhibits a dominant summer low flow regime. Precipitation enters the area  
2 from the Northwest through Atlantic cyclones, although screened to some extent by the Alps,  
3 as well as from the South through Mediterranean cyclones. Precipitation and air temperature  
4 are important for low flows. The region is represented by the Zollfeld catchment at the Glan  
5 (432 km<sup>2</sup> area, 453 m altitude). The Buwe region (for Bucklige Welt) is located in the Southeast  
6 of Austria in the lee of the Alps, at the transition to a Pannonic climate. The precipitation is  
7 lowest in this region. Low flows mainly occur in summer with precipitation and air temperature  
8 as important controls. The region is represented by the Altschlaining catchment at the  
9 Tauchenbach (89 km<sup>2</sup> area, 316 m altitude). Streamflow records in the four catchments over the  
10 period 1976-2008 were used for all three pillars.

11 Climate records were used for the second and third pillars. Gridded data sets of daily  
12 precipitation, air temperature and potential evaporation over the period 1976-2008 were used  
13 for calibrating the hydrological model. These data are based on measured daily precipitation at  
14 1091 stations and daily air temperature at 212 stations. Potential evaporation was estimated by  
15 a modified Blaney–Criddle method based on daily air temperature and potential sunshine  
16 duration (Parajka et al., 2007). For each catchment, precipitation and temperature records at  
17 one representative station over the period 1948-2010 were analysed as a basis of the stochastic  
18 simulations (third pillar).

19

## 20 **4 Methods used for the pillars**

### 21 **4.1 Extrapolation of observed low flow trends**

22 The stream flow records of the four stream gauges were analysed to estimate  $Q_{95}$  low flow  
23 quantiles (i.e. the flow that is exceeded 95% of the time) for each year. The serial correlations  
24 of these annual low flow series were mostly insignificant, so they were not prewhitened (Yue  
25 et al., 2002). Trends were tested for significance by a standard Mann-Kendall test. The trends  
26 were estimated as the medians of all slopes between pairs of sample points (Sen's slope, Sen,  
27 1968) with regression parameters  $\hat{a}$  and  $\hat{b}$ :

$$28 \quad \hat{Q}_{95}(t_0) = \hat{a} + \hat{b}t_0 \quad (1)$$

29 The uncertainty of the trends was assessed by a nonparametric bootstrapping approach, which  
30 provides accurate confidence bounds in the case of non-Gaussian regression residuals (Efron  
31 and Tibshirani, 1993). The approach simulates the uncertainty distribution of trend estimate at  
32 time  $t_0$  by resampling 5000 replications from the annual  $Q_{95}$  series and calculating the  
33 regression parameters  $\hat{a}$  and  $\hat{b}$  for each of them. Equation (1) applied to these parameter  
34 distributions yields the uncertainty distribution of trend estimate at time  $t_0$ , and its 0.025 and  
35 0.975 empirical quantiles constitute the bounds of a two-sided 95% confidence interval.

36 For the purpose of this paper we assumed that the trends are linear and persistent, and so  
37 extrapolated them into the future. This is of course a strong assumption less likely to be valid  
38 with increasing time horizon.

### 39 **4.2 Climate projections and runoff modelling**

40 Four regional climate model (COSMO-CLM) runs were selected from the reclip:century 1  
41 project (Loibl et al., 2011) forced by ECHAM5 and HADCM3 GCMs for three IPCC emission  
42 scenarios (A1B, B1 and A2). These scenarios were selected for consistency with other ongoing

1 studies in Austria (e.g. Parajka et al., 2016). In order to check their realism with respect to  
 2 droughts and low flows, the Standardized Precipitation Evaporation Index, SPEI (Vicente-  
 3 Serrano et al., 2010) was evaluated, which is the Gaussian-transformed standardized monthly  
 4 difference of precipitation and evaporation. Values below zero indicate deficits in the climatic  
 5 water balance, and values below -1 indicate drought conditions. The SPEI has been adopted  
 6 here for its simplicity and because it can be calculated from the HISTALP data (Auer et al.,  
 7 2007) back to the year 1800. Haslinger et al. (2014) demonstrated that the SPEI is correlated  
 8 well with summer low flows in the study region. In the winter (Fig. 1, bottom panels), the  
 9 simulations (light red lines) for Hoalpe and Muhlv seem to be more consistent with decadal  
 10 observed fluctuations from the HISTALP data set (red lines) than for Gurk and Buwe. Note that  
 11 the comparison should focus on the long term (decadal) dynamics rather than individual years  
 12 due to the nature of the climate simulations. Overall, SPEI remains rather stable which is due  
 13 to little change in winter precipitation. In the summer (Fig. 1, top panels), the simulations are  
 14 somewhat less consistent with the observations than for the winter, in particular for Buwe where  
 15 the simulations show a decreasing trend in the overlapping period (1961-2003) while the  
 16 observations show little change. Overall, the summer SPEI projections show a decreasing trend  
 17 indicating a dryer future and the trend tends to steepen beyond 2050. This is mainly due to the  
 18 precipitation characteristics of the ECHAM5 simulations used and not reflected in the other  
 19 models or ECHAM5 runs. The extremely negative trends in the summer SPEI should therefore  
 20 be treated with caution.

21 Runoff is simulated by the delta change approach (e.g. Hay et al., 2000; Diaz-Nieto and Wilby,  
 22 2005). A conceptual rainfall runoff model (TUWmodel) is used here which simulates the daily  
 23 water balance components from precipitation, air temperature and potential evaporation inputs  
 24 (Viglione and Parajka, 2014; Parajka et al., 2007; Ceola et al., 2015). The routing component  
 25 of the model, which is most relevant for low flows, consists of a number of reservoirs with  
 26 different storage coefficients. Specifically, excess rainfall enters the upper zone reservoir and  
 27 leaves this reservoir through three paths: outflow from the reservoir based on a fast storage  
 28 coefficient; percolation to the lower zone with a constant percolation rate; and, if a threshold of  
 29 the storage state is exceeded, through an additional outlet based on a very fast storage  
 30 coefficient. Water leaves the lower zone based on a slow storage coefficient. The model  
 31 parameters (including the reservoir parameters representing groundwater storage) were  
 32 calibrated against observed streamflow by the SCE-UA procedure (Parajka et al., 2007; Duan  
 33 et al., 1992). The objective function ( $Z_Q$ ) was chosen on the basis of prior analyses in the study  
 34 region (Parajka and Blöschl, 2008) as

$$35 \quad Z_Q = w_Q \cdot M_E + (1 - w_Q) \cdot M_E^{log} \quad (2)$$

36 where  $w_Q$  and  $(1 - w_Q)$  are the weights on high and low flows, respectively, and  $M_E$  and  $M_E^{log}$   
 37 are estimated as

$$38 \quad M_E = 1 - \frac{\sum_{i=1}^n (Q_{obs,i} - Q_{sim,i})^2}{\sum_{i=1}^n (Q_{obs,i} - \overline{Q_{obs}})^2} \quad (3)$$

$$39 \quad M_E^{log} = 1 - \frac{\sum_{i=1}^n (\log(Q_{obs,i}) - \log(Q_{sim,i}))^2}{\sum_{i=1}^n (\log(Q_{obs,i}) - \overline{\log(Q_{obs})})^2} \quad (4)$$

1  $Q_{obs,i}$  is the observed discharge on day  $i$ ,  $\overline{Q_{obs}}$  is its average over the calibration (or verification)  
2 period of  $n$  days, and  $Q_{sim,i}$  is the simulated discharge.

3 In order to assess the uncertainty of low flow projections from a hydrological modelling  
4 perspective, different calibration variants were evaluated by varying the weights of Eq. (2),  
5 following the methodology of Parajka et al. (2016). In order to assess the impact of time stability  
6 of the model parameters, the model was calibrated separately for three different periods (1976-  
7 1986, 1987-1997, 1998-2008), following the methodology of Merz et al. (2011).

8 Air temperatures and precipitation of the four regional climate model runs were then evaluated  
9 for a reference period (1976-2008) and compared with two future periods (2021-2050 and 2051-  
10 2080) for each month separately. The differences (delta) were added to the observed daily air  
11 temperatures and precipitation values for the four catchments from which future stream flow  
12 was simulated using the rainfall-runoff model.

### 13 **4.3 Extrapolation of stochastic rainfall characteristics and runoff modelling**

14 A stochastic model is used to investigate what would happen if the trend of observed  
15 precipitation and air temperature characteristics in the period 1948-2010 would persist into the  
16 future. The results of the stochastic model are used to drive a lumped version of the TUWmodel  
17 which is similar to the one used in the delta-change approach.

18 The precipitation model is the point model of Sivapalan et al. (2005) which simulates discrete  
19 rainfall events whose storm durations, interstorm periods and average event rainfall intensities  
20 are all random, governed by specified distributions whose parameters vary seasonally. The  
21 model was run on a daily time step without considering within-storm rainfall patterns as the  
22 interest was in low flows. A storm-separation algorithm was applied to the precipitation data of  
23 the four stations, based on a minimum duration of dry periods, in order to isolate precipitation  
24 events. From the event time series the temporal trends of three model parameters (mean annual  
25 storm duration, mean annual inter-storm period and mean annual storm intensity) were  
26 estimated by the Theil-Sen algorithm, to serve as the trend components of the precipitation  
27 model. The trends in these precipitation model components were subsequently extrapolated into  
28 the future. Similar to the low flow extrapolation, this is a strong assumption less likely to be  
29 valid with increasing time horizon. The remaining rainfall model parameters were calibrated to  
30 the precipitation data as described in Viglione et al. (2012) and were kept constant for the entire  
31 simulation period. The stochastic rainfall model was finally used to simulate an ensemble of  
32 100 possible time series of precipitation affected by trends in the three model parameters for  
33 the period 1948-2080.

34 For air temperature, instead, 100 possible time series were obtained by randomising the  
35 observations in the following way. The time series of daily temperatures were detrended  
36 according to the observed trend of mean annual temperatures, the years were randomly mixed  
37 (with repetition), and the trend was added to the reshuffled series. The trend in the temperatures  
38 was reflected by an analogous trend in potential evaporation.

39

## 40 **5 Results**

### 41 **5.1 Extrapolation of observed low flow trends**

42 Table 1 summarizes the results of the trend analyses of  $Q_{95}$  low flows. The Hoalp catchment  
43 exhibits a significantly increasing trend indicating that the catchment has become wetter over

1 the observation period while the Buwe catchment indicates a significantly decreasing trend.  
2 Muhlv and Gurk show decreasing trends which are, however, not significant at the 0.05 level.

3 While our focus is on the four example catchments, it is important to put the local analyses in  
4 a regional context to avoid the detection of local effects on the flow regime, such as  
5 anthropogenic impacts. Equally important, the regional context assists in a more meaningful  
6 interpretation of regional climate scenarios that are valid for footprints of a few hundreds of  
7 square kilometres or more. Figure 2 shows the trends of the four example catchments together  
8 with trends of 408 stream gauges in Austria and neighbouring regions. The trend patterns are  
9 in line with the main hydro-climatic units represented by the four catchments. Significantly  
10 increasing trends (large blue points) such as in the Hoalp catchment are generally found in the  
11 Alpine region. Decreasing trends (large red points) occur north of the Alps and, more  
12 frequently, in the Southeast of Austria. Additional regional analyses (not shown here), including  
13 field significance testing, confirm the finding that the decreasing trends in the Southeast are  
14 more significant than in the North. The Buwe region appears to be particularly affected by  
15 climate change as low flows show a strong decrease at the end of the observation period.

16 Table 2 presents the trend extrapolations together with their confidence bounds. Extrapolating  
17 observed trends to 2021-2050 would give a 39% increase in  $Q_{95}$  for Hoalp, but the uncertainty  
18 is large, as indicated by a range of the confidence interval from -7 to 71%. Trend extrapolations  
19 for the other catchments result in decreases which are smallest in Muhlv (-8%), moderate in  
20 Gurk (-36%) and largest in Buwe (-90%). The uncertainty range is large, e.g. -41% to +34%  
21 for Muhlv, which is almost ten times the mean change. Clearly, trend extrapolations involve a  
22 lot of uncertainty, and this uncertainty increases as one moves to the more distant time horizon  
23 of 2051-2080 (Table 2), including negative discharges for Buwe and Gurk indicating  
24 intermittent behaviour. Obviously, one would have very low confidence in the absolute figures  
25 of such trend scenarios for the more distant future.

## 26 **5.2 Climate projections and runoff modelling**

27 Table 3 summarizes the runoff model efficiencies  $Z_Q$  for different weights in the objective  
28 function.  $w_Q = 0$  emphasises low flows, while  $w_Q = 1$  emphasises high flows in the calibration.  
29 With the exception of Gurk, there is a clear trend of increasing (calibration) model performance  
30 from high flows to low flows. The model performance between the calibration decades varies  
31 little. Overall, Hoalp gives the largest efficiency which is a reflection of the strong seasonality  
32 associated with snow storage and melt while Buwe gives the lowest efficiency due to the flashy  
33 nature of runoff that is difficult to model on a daily time step (Fig. 3). The flashy runoff response  
34 of Buwe is related to shallow soils, efficient drainage and frequent convective storms (see Gaál  
35 et al., 2012). Additionally, there are only two climate stations in the Buwe catchment, so local  
36 precipitation events may not always be captured well. The event variability is large between  
37 and within the years (Fig. 3). Both low flows and floods mainly occur in summer. As compared  
38 to other catchments in Austria (Parajka et al., 2016), the Hoalp and Buwe catchments represent  
39 typical conditions of high and low model performances, respectively.

40 Figure 4 left shows the simulated annual  $Q_{95}$  low flows for the reference period 1976-2008,  
41 based on calibrations for two subperiods (yellow and blue), in each case indicating the  
42 variability of  $Q_{95}$  due to 11 calibration variants with different weights  $w_Q$  in the objective  
43 function (Table 3). The right panels show the simulations for two sets of weights (light orange  
44 and red), in each case indicating the variability of  $Q_{95}$  due to model parameters obtained from  
45 different decades. Although the model has not specifically been calibrated to  $Q_{95}$ , it simulates  
46  $Q_{95}$  rather well. The differences between the two weighting variants (Fig. 4 right) are small in

1 absolute terms. The effect of temporal instability of the model parameters is clearly visible in  
2 Buwe and Gurk (Fig. 4 left), as the model calibrated to the 1976-1986 period tends to  
3 overestimate  $Q_{95}$  in the period 1998-2008. The decade 1976–1986 represents a colder period  
4 with less evaporation and relatively higher runoff generation rates which is reflected by lower  
5 values of the soil moisture storage parameter (FC) and lower values of the parameter controlling  
6 runoff generation (BETA). The model therefore overestimates runoff when applied to the drier  
7 and warmer period 1998–2008. Even though Table 3 indicates that Buwe has the lowest model  
8 performance, this is not reflected in the  $Q_{95}$  low flow simulations in Fig. 4. This is because the  
9 model does not simulate the fast runoff fluctuations well, however, it does much better with  
10 prolonged drought spells.

11 Figure 4 also shows that the uncertainty of  $Q_{95}$  estimates is largest in the Hoalp. The seasonal  
12 runoff variability of Alpine rivers is larger than that of low-land rivers which makes the model  
13 calibration more sensitive to the weights assigned to high and low flows. Hoalp is also more  
14 sensitive to the choice of the calibration period which is a reflection of the high sensitivity of  
15 low flows to seasonal climate. In contrast, the uncertainty is smallest in the Gurk and Buwe  
16 catchments where the effect of time variability of the model parameters is of similar magnitude  
17 as the effect of the weights in the objective function.

18 Scenarios of air temperature and precipitation from the four climate model runs are presented  
19 in Fig. 5. The largest warming is obtained by HADCM3 with an increase of more than 2°C in  
20 January and the summer months. In January the ECHAM5-A2 run simulates a decrease in air  
21 temperature, while the other runs simulate an increase. The ECHAM5 scenarios are consistent  
22 for the summer months with an increase in air temperature of about 1°C. The precipitation  
23 projections are regionally less consistent and vary mostly around  $\pm 15\%$ . Exceptions are the  
24 HADCM3 run which simulates a decrease of almost 30% in the Gurk and Buwe catchments in  
25 August, and the ECHAM5-A1B run which simulates an increase of about 30% in the Hoalp  
26 and Muhlv catchments in December.

27 The delta change projections for the period 2021-2050 relative to simulated runoff in the  
28 reference period are shown in Fig. 6. They indicate an increase of annual  $Q_{95}$  low flows in the  
29 Alpine Hoalp catchment which is in the range of 15 to 30% and 20 to 45% for the different  
30 climate projections and calibration weights, respectively. In the Muhlv catchment, changes are  
31 small, while for Gurk and Buwe decreases are projected which are around 7-13% and 15-20%,  
32 respectively.  $Q_{95}$  is not only sensitive to the selection of the climate scenarios, but also to the  
33 selection of the objective function and the calibration period. The uncertainty is largest in the  
34 Hoalp catchment, where the objective function is more important than choice of the climate  
35 scenarios. The mean winter air temperature in Hoalp is about -6.0°C which is projected to  
36 increase by 2 to 2.5°C, depending on the scenario. These differences are of little relevance for  
37 snow storage and snowmelt runoff during the winter low flow period. Muhlv and Buwe are also  
38 sensitive to the choice of objective function and calibration period, while for the Gurk the choice  
39 of climate scenario is more important.

### 40 **5.3 Extrapolation of stochastic rainfall characteristics and runoff modelling**

41 Figure 7 shows that the estimated trend components fit well to the precipitation statistics.  
42 Annual mean storm duration decreases quite strongly for the Hoalp (by about -0.8 days / 100  
43 yrs). There is also a slight decrease for Gurk (-0.4 days / 100 yrs) and Buwe (-0.3 days / 100  
44 yrs). Interstorm period and storm intensity (Fig. 7, centre and right panels) show no significant  
45 changes, apart from the Gurk where the annual mean interstorm period increases by about 1



1 day / 100 yrs, and annual mean storm intensity increases by 2 mm/day per 100 yrs (which is a  
2 30% increase per 100 yrs).

3 The stochastic simulations (Fig. 8) indicate no trends in mean annual precipitation for Muhlv  
4 in the North and Gurk in the South of Austria, a drying trend for Buwe in the Southeast and  
5 Hoalp in the Alps, but in the latter case the observations exhibit a rather complex signal which  
6 is not well represented by the linear model. The simulated temperatures (Fig. 8, right panels)  
7 are more consistent with the observations with a persistently increasing trend in all catchments.  
8 The trend is most pronounced in the Alps (+4.4 °C / 100 yrs), somewhat less pronounced in the  
9 South and Southeast (+2.8 and +2.6 °C / 100 yrs), and there is only a weak trend in the North  
10 (+1.7 °C / 100 yrs) of Austria.

11 Figure 9 shows the stochastic projections of annual runoff and  $Q_{95}$  low flows (red lines) together  
12 with the observations (black lines). For Hoalp (top row)  $Q_{95}$  decreases only slightly despite the  
13 simulated large decrease of annual runoff and precipitation. This is because winter low flows  
14 are more controlled by air temperatures which increase the low flows, and the two effects  
15 essentially cancel. For Muhlv (second row in Fig. 9), the model extrapolates a slight reduction  
16 of  $Q_{95}$  in the future, even though there is hardly any change in the annual precipitation (second  
17 row in Fig. 8), which is due to increases in the evaporation. For Gurk (third row in Fig. 9), the  
18 model also extrapolates a slight decrease in  $Q_{95}$  which is a result of the increasing trends in both  
19 evaporation and the interstorm period (Fig. 7 and 8). For Buwe (bottom row in Fig. 9), the  
20 extrapolations yield a moderately decreasing trend of  $Q_{95}$  which results from the combined  
21 effect of slightly decreasing precipitation and increasing evaporation.

22 The underlying assumption of observed trends in precipitation and temperature to persist into  
23 the future is quite strong. In contrast to the other pillars, here we do not consider the uncertainty  
24 associated with the estimation (and extrapolation) of the trends. The confidence bounds in Fig.  
25 9 and 10 represent the modelled variability of the low-flow producing processes, which are  
26 assumed to be known both in the present and in the future. Despite the strong assumptions made  
27 it should be noted that the results of this approach are non-trivial, as the way the trends in  
28 precipitation and temperature translate into trends in low-flows differs between the catchments  
29 because of nonlinear process interactions.

30

## 31 **6 Three-pillar synthesis**

### 32 **6.1 Combination of information**

33 The concept of multi-model ensembles starts from the premise that (a) a group of model  
34 projections will give more reliable results than the individual models alone and (b) the  
35 consistency/inconsistency of the model results is an indicator of the robustness or reliability of  
36 the projections (Knutti et al., 2010). In the context of the three-pillar approach proposed here,  
37 the methods and information used in each pillar are largely independent from each other, so one  
38 would expect the errors to be close to independent, and a combination of the projections should  
39 indeed increase the overall reliability of the projection. We will evaluate heuristically to what  
40 degree this premise can be achieved based on hydrological reasoning and visual comparisons  
41 of synoptic plots of the individual estimates and their respective confidence bounds. The  
42 reasoning accounts for the differences in the nature of the uncertainties of the projections and  
43 gives more weight to the more reliable pieces of information.

44 When comparing the projections two cases exist. In the first case, projections are consistent  
45 within their confidence bounds. This will lend credence to all projections as they support each

1 other, in particular if the changes of the driving hydrological processes (precipitation, snow  
2 storage and melt, evaporation) are consistent. The overall uncertainty will be expressed here as  
3 three levels of confidence (high, medium, low) (Field and Intergovernmental Panel on Climate  
4 Change, 2012). In the second case, the individual projections are not consistent within their  
5 uncertainty bounds which will suggest lower confidence in the overall projections. Rather than  
6 simply averaging the individual projections, here, we explore the reasons for the disagreement,  
7 by checking the credibility of each projection based on the data used and the assumptions made.

## 8 **6.2 Application to the study area**

9 Figure 10 compiles the  $Q_{95}$  projections from the three pillars, and Fig. 11 shows their probability  
10 density functions for the period 2021-2050.

11 For the Hoalp region in the Alps (Fig. 10, top left), both the extrapolation of observed low flow  
12 trends and the climate scenarios suggest increases in low flows. In this region, low flows occur  
13 in winter due to snow storage processes which are mainly driven by seasonal temperature (Fig.  
14 3). Schöner et al. (2012) showed that regional climate models are able to simulate the observed  
15 increase of winter temperatures in the Alpine region since the 1970s well, which suggests that  
16 the winter low flow changes are captured well by the climate scenarios. However, a lot of  
17 uncertainty is introduced by the parameterisations of the rainfall-runoff model as indicated by  
18 the wide boxes in Fig. 10. This uncertainty is due to the sensitivity of the simulations to the  
19 model parameters in an Alpine environment (Fig. 4 and 6). From a regional perspective (Fig.  
20 2), the observed low flow trends are significant, i.e. the percentage of stations with a significant  
21 trend is much greater than expected by chance (Blöschl et al., 2011). This means that the climate  
22 scenarios and the trend extrapolations can be reconciled, at least in terms of the sign of the  
23 changes. The stochastic extrapolations, in contrast, project no or even slightly decreasing low  
24 flow trends. A closer inspection of observed air temperatures suggests that winter temperatures  
25 ( $+0.65\text{ }^{\circ}\text{C}/10\text{ yrs}$ ) have changed more by half than the annual average ( $+0.46\text{ }^{\circ}\text{C}/10\text{ yrs}$  in the  
26 period 1976-2010). However, the stochastic model assumes a constant change throughout the  
27 year which results in underestimates of future  $Q_{95}$ . Of course, the model could be  
28 straightforwardly extended to include seasonal variations in the changes but, as it is now, it  
29 nicely illustrates the case of an inconsistency that is well understood. Because of this, little  
30 weight is given to the stochastic projections in the overall assessment, and one would expect an  
31 increase in low flows by at least 20-40% for the 2020-2050 period with medium to high  
32 confidence.

33 For the Muhlv region north of the Alps, the extrapolation of observed low flow trends  
34 corresponds well with the stochastic projections (Fig. 10 top right). Both methods project a  
35 slight reduction of about 5-10% for 2021-2050. Seasonal air temperature trends are similar to  
36 the annual trends ( $0.43\text{ }^{\circ}\text{C}/10\text{ yrs}$  in the period 1976-2010), so the structure of the stochastic  
37 model is appropriate here. The rainfall-runoff simulations capture the observed trend well for  
38 the observation period. The climate scenarios predict a slight decrease in  $Q_{95}$  for 2021-2050 but  
39 there is a lot of variability between the scenarios (also see Fig. 5). On a regional level, Blöschl  
40 et al. (2011) reported no field significance of the observed low flow trends in this region which,  
41 together with the three pillars here suggests a slight tendency for decreasing low flows in 2020-  
42 2050 with medium confidence. For the 2050-2080 period all methods become more uncertain,  
43 but all point towards a drying trend (low to medium confidence).

44 The Gurk region south of the Alps (Fig. 10 bottom left) shows a somewhat similar behaviour  
45 to Muhlv, although the observed low flow pattern is rather nonlinear with a drop at the  
46 beginning of the observations and a flattening out after 1990. Extrapolating a linear trend in

1 low flows may therefore not be reliable. The stochastic projections are more in line with the  
2 observations, and indicate a slight decrease until 2080. Winter SPEI in the period 1961-2003 is  
3 not simulated well (Fig. 1) which suggests issues with the seasonal water balance of the GCM  
4 based simulations. However, the climate scenario projections are in line with extrapolated  
5 trends and stochastic projections. All pillars point to a slight to moderate drying trend in low  
6 flows for the 2020-2050 period (medium confidence) and towards a somewhat stronger drying  
7 trend for 2050-2080 (low to medium confidence).

8 The Buwe region in the South-east gives larger changes (Fig. 10, bottom right). The observed  
9 low flow trends are strongly influenced by the recent dry years between 2000 and 2005 which  
10 is consistent with the regional behaviour (Fig. 2 and Blöschl et al. (2011)). A linear trend  
11 extrapolation, however, does not seem very plausible, in particular because the most recent year  
12 in the data set (2008) was less dry. In fact, more recent data for 2009-2014 (not included in the  
13 analysis) show that low flows have partly recovered (annual Q95 values ranging from 0.1 to  
14  $0.3 \text{ m}^3\text{s}^{-1}$ ) illustrating the limitations of trend extrapolation. The stochastic projection yields a  
15 moderately decreasing trend, which is more plausible, and related to both increasing  
16 temperatures and decreasing precipitation (Fig. 8). The climate scenarios give slightly stronger  
17 decreasing trends for the two periods, but it should be noted that, in contrast to the other  
18 catchments, the summer SPEI trend in the period 1961-2003 is not captured well and likely  
19 overestimated by the climate simulations (Fig. 1, top right). Fig. 2 shows consistently  
20 decreasing trends of observed streamflow in the region. Overall, the pillars therefore point  
21 towards a slight to moderate drying trend for 2020-2050, and a stronger drying trend for 2050-  
22 2080 with medium confidence.

## 24 7 Discussion

### 25 7.1 Extrapolation of observed low flow trends

26 The trend scenarios are based on the assumption that changes are linear over time. This is a  
27 simplifying view of non-stationarity. The Earth system is clearly non-linear, so often regime  
28 shifts are observed rather than trends. These can be detected in a similar way as trends (see,  
29 e.g., Rodionov, 2006) but it is more difficult to make assumptions of persistence of change than  
30 for the case of linear trends. In the European Alps, annual air temperatures have increased  
31 linearly since the mid-1970s, so a continuing trend is a plausible assumption for the near future.  
32 Trends in air temperatures translate into changes in low flows in a non-linear way and this  
33 depends on the time of the year low flows occur (Laaha and Blöschl, 2006). Winter low flows  
34 are a consequence of frost and snow storage, which is reflected by a remarkable co-behaviour  
35 of observed low flows with temperature for the Alpine Hoalp catchment (Fig. 10 top left).

36 For the other catchments that exhibit a summer low flow regime, the past changes of low flows  
37 are more subtle. The flow records are rather short, so discerning trends from long range  
38 fluctuations is difficult (Montanari et al., 1997). In all cases, the uncertainty of the trend  
39 scenarios is large, as indicated by the wide confidence bounds. It should be noted that the  
40 confidence bounds are conditional on the assumption that the linear trend model applies. If one  
41 relaxed this assumption, the bounds would be even wider. Part of the uncertainty comes from  
42 the relatively short record length (33 years). Hannaford et al. (2013) showed that low flow  
43 trends in European regimes are subject to pronounced decadal-scale variability so that even  
44 post-1960 trends (50 years) are often not consistent with the long-term pattern. Long climate  
45 records may assist in trend detection. Haslinger et al. (2014) found that the Standardized  
46 Precipitation Evaporation Index (SPEI) is a good proxy of summer low flows in the study area

1 where the HISTALP data set (Auer et al., 2007) allows analysing climate fluctuations back to  
2 the year 1800 (Fig. 1). The decreasing trends of summer SPEI from the climate projections (Fig.  
3 1) are in line with the low flow trends in Muhlvi and Gurk, and both point to a decrease of low  
4 flows that extends into the future.

## 5 **7.2 Climate projections and runoff modelling**

6 Similar to the ensemble projections of Wong et al. (2011), Majone et al. (2012) and De Wit et  
7 al. (2007) we assessed the uncertainty arising from the choice of the climate model and emission  
8 scenario. We did not assess downscaling errors, as De Wit et al. (2007) did, as they usually play  
9 a minor role when using a delta change approach that applies a change factor to locally observed  
10 signals. Uncertainty arising from the hydrological model structure may also be assessed by a  
11 model ensemble (e.g. Habets et al., 2013) but we have chosen to focus on the uncertainty of  
12 model parameters instead. The results suggest that the Q<sub>95</sub> projections are not only sensitive to  
13 the choice of climate scenarios, but also to the objective function and the calibration period.  
14 The uncertainty associated with the objective function is largest in the Alpine Hoalp catchment,  
15 where the strong streamflow seasonality makes the weighting between high and low flows  
16 particularly important. The uncertainty associated with the calibration period is largest in Buwe  
17 and Gurk where parameters from a colder period with less evaporation tend to overestimate  
18 runoff in warmer periods. A similar effect is expected for a future, warmer climate, so the  
19 projected low flows may decrease more strongly than the projected average. This finding may  
20 depend both on model type and the climate region. Hay et al. (2000), for example, found a  
21 minor role of the hydrological model for three river basins in the US, although they did not  
22 specifically examine the time stability of model parameters. Bosshard et al. (2013), on the other  
23 hand, suggested that the hydrological model accounted for 5–40% of the total streamflow  
24 ensemble uncertainty in the Alpine Rhine. Similarly, Samaniego et al. (2013) found that  
25 accounting for hydrological model parameter uncertainty is essential for identifying drought  
26 events, and multi-parameter ensembles were efficiently able to identify the magnitude of that  
27 uncertainty.

28 Low flow projections are challenging because low flows are typically driven by groundwater  
29 discharge processes (both recharge and discharge). These processes are difficult to understand  
30 and model due to their local nature. Fleckenstein et al. (2006), for example, found that the  
31 percentage of river channel responsible for 50% of total river seepage during low flow  
32 conditions in the Cosumnes River, California ranged from 10 to 26% depending on the spatial  
33 configuration of hydrogeologic heterogeneity. This heterogeneity has not been resolved in the  
34 present study and is rarely resolved in catchment scale climate assessment studies. It is therefore  
35 important to note that, while the climate drought processes tend to be rather large scale, the  
36 catchment response during low flow periods can have specific local effects which differ from  
37 those of the larger scale pattern.

## 38 **7.3 Extrapolation of stochastic rainfall characteristics and runoff modelling**

39 Stochastic models of rainfall characteristics can be conditioned to future climates in a number  
40 of ways (see, e.g. Hall et al., 2014). A common method is to first calibrate the model parameters  
41 to the current climate and then adjust the parameters to precipitation from climate scenarios at  
42 daily, seasonal and annual time scales (e.g. Hundecha and Merz, 2012; Blöschl et al., 2011). To  
43 illustrate the three-pillar approach we have adopted here the very simple assumption of  
44 extrapolating the trends in the rainfall model parameters and air temperatures linearly into the  
45 future. The reasoning, and the limitations, are similar to the direct trend extrapolation of low

1 flows, building on the inertia of the climate system. Consequently, the extrapolation of  
2 temperature will be more appropriate than that of precipitation and the extrapolation into the  
3 near future will be more appropriate than that into the more distant future.

4 Alternative stochastic models could be used within the same three-pillar framework. The model  
5 could be adjusted to climate scenarios in a similar way as the model of Hundsdoerfer and Merz  
6 (2012), and correlations between precipitation and air temperature could be accounted for. Also,  
7 the long range dependence of streamflow (Szolgayová et al., 2014) could be considered by  
8 extending the stochastic precipitation model (e.g. Thyer and Kuczera, 2003). This will result in  
9 more complex patterns of future simulated low flows.

#### 10 **7.4 Assessing the value of synthesis**

11 Climate impact and assessment studies in hydrology have traditionally been dominated by the  
12 paradigm of modelling cascades (Blöschl and Montanari, 2010), so a fresh look at the problem  
13 for the particular case of low flows opens up a number of opportunities. The three pillar  
14 approach allows for a diverse set of methods based on different assumptions and data to be  
15 compared and combined in a coherent way. For the case study catchment Muhlv in the region  
16 north of the Alps, for example, consistently small low flow changes are projected by all methods  
17 which adds credence to the projections. The synthesis framework proposed here puts a lot of  
18 emphasis on heuristic process reasoning. This may contribute to a better understanding of low  
19 flow response to a future climate than a mere examination of scenario results. For an alpine  
20 region such as Austria the key to understanding low flows is whether they are controlled by  
21 freezing and snow melt processes, or by the summer moisture deficit associated with  
22 evaporation. Understanding of the key processes helps putting the projections from the diverse  
23 methods into perspective. For example, for the Alpine Hoalpe catchment this reasoning points  
24 towards increasing low flows which is also consistent with all three pillars adopted here. In a  
25 similar way, Luce and Holden (2009) and Luce et al. (2013) explained decreasing low flow  
26 trends in the Pacific Northwest of the US by declines in mountain precipitation and suggested  
27 that this trend will persist into the future. Luce et al. (2013) pointed out that in their study initial  
28 interpretations of apparently consistent trends would have been misleading, partly due to  
29 artifacts in data, missing information and overextrapolation of trends, which triggered  
30 additional analyses leading to a differing perception of hydrological change. This example  
31 illustrates the importance of careful process reasoning in every step of the analysis.

32 The three pillar approach also provides opportunities for a more complete assessment of the  
33 uncertainty of the projections. The multi-model ensemble premise of variations between  
34 ensemble members being an indicator of projection uncertainty is consistent with the case study  
35 findings of this paper. For example, the comparisons of the methods for the Hoalpe catchment  
36 highlighted issues with the assumption of a uniform seasonal temperature change of the  
37 stochastic model, so less credibility was given to this pillar in this particular case. For the Buwe  
38 catchment, non-linear changes of observed low flows shed doubts on the linear-trend  
39 assumption, so less credibility was given to the low flow extrapolation pillar. On the other hand,  
40 for predicting near-future low flows in the Hoalpe catchment, the trend extrapolation appears  
41 most reliable. From trend extrapolations alone one would infer a 39% increase in low flows  
42 until 2021-2050 (Table 2) but the uncertainty is of equal magnitude. Additional information  
43 from rainfall runoff projections that suggest an increase of up to 30% constrain the projected  
44 increase to about 20 to 40%.

45 In the context of water resources management, decision makers are usually reluctant to use the  
46 output from black box models as the sole basis of their decisions. Just as important as the

1 expected changes in the water system are the uncertainties associated with the changes as well  
2 as a process reasoning in terms of cause and effect. This is particular the case if robust drought  
3 management strategies, such as the vulnerability approach, are to be adopted (Wilby and Dessai,  
4 2010; Blöschl et al., 2013). Typically, these strategies are designed to perform well over a wide  
5 range of assumptions about the future and potentially extremely negative effects. Central to the  
6 approach is an understanding of the cause-effect relationships within the water system under a  
7 variety of conditions, as well as an appreciation of the possible uncertainties. Methods often  
8 involve exploratory modelling approaches (Watts et al., 2012) which fit well with the three  
9 pillar approach proposed here. We therefore believe that the approach put forward in this paper  
10 can play an important role in assisting risk managers in developing drought management  
11 strategies for the practice.

12 It should be emphasised that the extrapolation pillars have been adopted here to illustrate the  
13 framework and could be replaced by other methods such as the “trading space for time”  
14 approach (Perdigão and Blöschl, 2014) where spatial gradients are transposed into temporal  
15 changes. Also, heuristic process reasoning has been adopted to compare the pillars based on  
16 expert judgement because of its flexibility. The combination could be based on formal methods  
17 (e.g. Bayesian methods, Viglione et al., 2013) that allow accounting for subjective information  
18 on low flows and their process causes. Finally, the three-pillar approach presented in this paper  
19 is not necessarily restricted to low flows and could be adapted to other hydrologic  
20 characteristics.

21

## 22 **8 Conclusions**

23 We propose a framework that combines low flow projections from different sources of  
24 information, termed pillars. To illustrate the framework three pillars have been chosen: (a)  
25 direct extrapolation of low flow trends (b) estimation of low flows from GCM-projected  
26 climates using a runoff model, and (c) stochastic simulations from trend-extrapolated climates  
27 using a similar runoff model.

28 The methods and information used in each pillar are largely independent from each other, so  
29 one would expect the errors to be close to independent, and a combination of the projections  
30 should increase the overall reliability of the projection. We evaluate heuristically to what degree  
31 this premise can be achieved for four example regions in Austria, based on hydrological  
32 reasoning and visual comparisons of synoptic plots of the individual estimates and their  
33 respective confidence bounds.

34 For the Alpine region where winter low flows dominate, trend projections and climate scenarios  
35 yield consistent projections of a wetting trend but of different magnitudes. For the region north  
36 of the Alps, all methods project rather small changes. For the regions in the South and Southeast  
37 more pronounced and mostly decreasing trends are projected but there is disagreement in the  
38 magnitude of the changes. The synthesis of the case study projections suggests that the  
39 framework (i) tends to enhance the robustness of the overall assessment, (ii) adds to the  
40 understanding of the cause-effect relationships of low flows, and (iii) sheds light on the  
41 uncertainties involved based on the consistency/inconsistency of the pillars.

42 Future work may be directed towards adding pillars, or replacing some of the pillars used here.  
43 One possibility is historic information from archives and tree ring analyses which would allow  
44 assessment of a wider spectrum of drought conditions. Other possibilities are the “trading space  
45 for time” approach as well as more formal multi-model ensembles.

46

## 1 **Acknowledgements**

2 The paper is a contribution to UNESCO's FRIEND-Water program. The authors would like to  
3 thank the Austrian Climate Research Program ACRP for financial support through the projects  
4 CILFAD (GZ B060362) and DALF-Pro (GZ B464822), and the Austrian Academy of Sciences  
5 for financial support through the 'Predictability of Runoff' project. We thank the Central  
6 Institute for Meteorology and Geodynamics (ZAMG) and the Hydrographical Service of  
7 Austria (HZB) for providing meteorological and hydrological data, and Tobias Gauster for  
8 assistance with Fig. 10. We would like to thank Luis Samaniego, Charlie Luce and Chuck Kroll  
9 for their useful comments on the manuscript.

10

## 11 **References**

- 12 Auer, I., Böhm, R., Jurkovic, A., Lipa, W., Orlik, A., Potzmann, R., Schöner, W., Ungersböck,  
13 M., Matulla, C., Briffa, K., Jones, P., Efthymiadis, D., Brunetti, M., Nanni, T., Maugeri, M.,  
14 Mercalli, L., Mestre, O., Moisselin, J.-M., Begert, M., Müller-Westermeier, G., Kveton, V.,  
15 Bochnicek, O., Stastny, P., Lapin, M., Szalai, S., Szentimrey, T., Cegnar, T., Dolinar, M., Gajic-  
16 Capka, M., Zaninovic, K., Majstorovic, Z. and Nieplova, E.: HISTALP—historical  
17 instrumental climatological surface time series of the Greater Alpine Region, *Int. J. Climatol.*,  
18 27(1), 17–46, doi:10.1002/joc.1377, 2007.
- 19 Blöschl, G. and Montanari, A.: Climate change impacts—throwing the dice?, *Hydrol. Process.*,  
20 24(3), 374–381, 2010.
- 21 Blöschl, G., Viglione, A., Merz, R., Parajka, J., Salinas, J. L. and Schöner, W.: Auswirkungen  
22 des Klimawandels auf Hochwasser und Niederwasser (Climate impacts on floods and low  
23 flows), *Österr. Wasser- Abfallwirtsch.*, 63(1-2), 21–30, 2011.
- 24 Blöschl, G., Viglione, A. and Montanari, A.: Emerging Approaches to Hydrological Risk  
25 Management in a Changing World, in *Climate Vulnerability*, pp. 3–10, Elsevier. [online]  
26 Available from: <http://linkinghub.elsevier.com/retrieve/pii/B9780123847034005050>  
27 (Accessed 3 November 2015), 2013.
- 28 Böhm, R., Auer, I., Brunetti, M., Maugeri, M., Nanni, T. and Schöner, W.: Regional  
29 temperature variability in the European Alps: 1760-1998 from homogenized instrumental time  
30 series, *Int. J. Climatol.*, 21(14), 1779–1801, doi:10.1002/joc.689, 2001.
- 31 Bosshard, T., Carambia, M., Goergen, K., Kotlarski, S., Krahe, P., Zappa, M. and Schär, C.:  
32 Quantifying uncertainty sources in an ensemble of hydrological climate-impact projections,  
33 *Water Resour. Res.*, 49(3), 1523–1536, doi:10.1029/2011WR011533, 2013.
- 34 Ceola, S., Arheimer, B., Baratti, E., Blöschl, G., Capell, R., Castellarin, A., Freer, J., Han, D.,  
35 Hrachowitz, M., Hundecha, Y., Hutton, C., Lindström, G., Montanari, A., Nijzink, R., Parajka,  
36 J., Toth, E., Viglione, A. and Wagener, T.: Virtual laboratories: new opportunities for  
37 collaborative water science, *Hydrol. Earth Syst. Sci.*, 19(4), 2101–2117, doi:10.5194/hess-19-  
38 2101-2015, 2015.
- 39 Chauveau, M., Chazot, S., Perrin, C., Bourgin, P.-Y., Sauquet, E., Vidal, J.-P., Rouchy, N.,  
40 Martin, E., David, J., Norotte, T., Maugis, P. and De Lacaze, X.: Quels impacts des  
41 changements climatiques sur les eaux de surface en France à l'horizon 2070 ?, *Houille Blanche*,  
42 (4), 5–15, doi:10.1051/lhb/2013027, 2013.

- 1 De Wit, M. J. M., Van den Hurk, B., Warmerdam, P. M. M., Torfs, P. J. J. F., Roulin, E. and  
2 Van Deursen, W. P. A.: Impact of climate change on low-flows in the river Meuse, *Clim.*  
3 *Change*, 82(3-4), 351–372, doi:10.1007/s10584-006-9195-2, 2007.
- 4 Diaz-Nieto, J. and Wilby, R. L.: A comparison of statistical downscaling and climate change  
5 factor methods: impacts on low flows in the River Thames, United Kingdom, *Clim. Change*,  
6 69(2-3), 245–268, 2005.
- 7 Douglas, E., Vogel, R. and Kroll, C.: Trends in floods and low flows in the United States:  
8 impact of spatial correlation, *J. Hydrol.*, 240(1-2), 90–105, 2000.
- 9 Duan, Q., Sorooshian, S. and Gupta, V.: Effective and efficient global optimization for  
10 conceptual rainfall-runoff models, *Water Resour Res.*, 28(4), 1015–1031, 1992.
- 11 Field, C. B. and Intergovernmental Panel on Climate Change: Managing the risks of extreme  
12 events and disasters to advance climate change adaptation: special report of the  
13 Intergovernmental Panel on Climate Change, Cambridge University Press, New York., 2012.
- 14 Fleckenstein, J. H., Niswonger, R. G., & Fogg, G. E. (2006). River-aquifer interactions,  
15 geologic heterogeneity, and low-flow management. *Ground water*, 44(6), 837-852.
- 16 Gaál, L., Szolgay, J., Kohnová, S., Parajka, J., Merz, R., Viglione, A. and Blöschl, G.: Flood  
17 timescales: Understanding the interplay of climate and catchment processes through  
18 comparative hydrology, *Water Resour. Res.*, 48(4), W04511, 2012.
- 19 Giuntoli, I., Renard, B., Vidal, J.-P. and Bard, A.: Low flows in France and their relationship  
20 to large-scale climate indices, *J. Hydrol.*, 482, 105–118, doi:10.1016/j.jhydrol.2012.12.038,  
21 2013.
- 22 Gupta, H.V., Blöschl, G., McDonnell, J., Savenije, H., Sivapalan, M., Viglione, A. and Wagener,  
23 T.: Synthesis. Chapter 12, in G. Blöschl, M. Sivapalan, T. Wagener, A. Viglione, H. Savenije  
24 (Eds.) *Runoff Prediction in Ungauged Basins - Synthesis across Processes, Places and Scales.*,  
25 pp. 361–383, Cambridge University Press, Cambridge, UK., 2013.
- 26 Gutknecht, D., Blöschl, G., Reszler, C. and Heindl, H.: Ein „Mehr-Standbeine“-Ansatz zur  
27 Ermittlung von Bemessungshochwässern kleiner Auftretenswahrscheinlichkeit, *Österr.*  
28 *Wasser- Abfallwirtsch.*, 58(3-4), 44–50, 2006.
- 29 Habets, F., Boé, J., Déqué, M., Ducharne, A., Gascoïn, S., Hachour, A., Martin, E., Pagé, C.,  
30 Sauquet, E., Terray, L., Thiéry, D., Oudin, L. and Viennot, P.: Impact of climate change on the  
31 hydrogeology of two basins in northern France, *Clim. Change*, 121(4), 771–785,  
32 doi:10.1007/s10584-013-0934-x, 2013.
- 33 Hall, J., Arheimer, B., Borga, M., Brázdil, R., Claps, P., Kiss, A., Kjeldsen, T. R.,  
34 Kriauciūnienė, J., Kundzewicz, Z. W., Lang, M., Llasat, M. C., Macdonald, N., McIntyre, N.,  
35 Mediero, L., Merz, B., Merz, R., Molnar, P., Montanari, A., Neuhold, C., Parajka, J., Perdigão,  
36 R. A. P., Plavcová, L., Rogger, M., Salinas, J. L., Sauquet, E., Schär, C., Szolgay, J., Viglione,  
37 A. and Blöschl, G.: Understanding flood regime changes in Europe: a state-of-the-art  
38 assessment, *Hydrol. Earth Syst. Sci.*, 18(7), 2735–2772, doi:10.5194/hess-18-2735-2014, 2014.
- 39 Hannaford, J. and Buys, G.: Trends in seasonal river flow regimes in the UK, *J. Hydrol.*, 475,  
40 158–174, 2012.
- 41 Hannaford, J., Buys, G., Stahl, K. and Tallaksen, L. M.: The influence of decadal-scale  
42 variability on trends in long European streamflow records, *Hydrol. Earth Syst. Sci.*, 17(7),  
43 2717–2733, doi:10.5194/hess-17-2717-2013, 2013.



- 1 Haslinger, K., Anders, I. and Hofstätter, M.: Regional climate modelling over complex terrain:  
2 an evaluation study of COSMO-CLM hindcast model runs for the Greater Alpine Region, *Clim.*  
3 *Dyn.*, 40(1-2), 511–529, 2013.
- 4 Haslinger, K., Koffler, D., Schöner, W. and Laaha, G.: Exploring the link between  
5 meteorological drought and streamflow: Effects of climate-catchment interaction, *Water*  
6 *Resour. Res.*, 50(3), 2468–2487, doi:10.1002/2013WR015051, 2014.
- 7 Hay, L. E., Wilby, R. L., Leavesley, G. H. and others: A comparison of delta change and  
8 downscaled GCM scenarios for three mountainous basins in the United States., *J. Am. Water*  
9 *Resour. Assoc.*, 36(2), 387–397, 2000.
- 10 Hundecha, Y. and Merz, B.: Exploring the relationship between changes in climate and floods  
11 using a model-based analysis, *Water Resour. Res.*, 48(4) [online] Available from:  
12 <http://onlinelibrary.wiley.com/doi/10.1029/2011WR010527/pdf> (Accessed 3 November 2015),  
13 2012.
- 14 Hurkmans, R., Terink, W., Uijlenhoet, R., Torfs, P., Jacob, D. and Troch, P. A.: Changes in  
15 streamflow dynamics in the Rhine basin under three high-resolution regional climate scenarios,  
16 *J. Clim.*, 23(3), 679–699, 2010.
- 17 Knutti, R., G. Abramowitz, M. Collins, V. Eyring, P.J. Gleckler, B. Hewitson, and L. Mearns,  
18 2010: Good Practice Guidance Paper on Assessing and Combining Multi Model Climate  
19 Projections. In: Meeting Report of the Intergovernmental Panel on Climate Change Expert  
20 Meeting on Assessing and Combining Multi Model Climate Projections [Stocker, T.F., D. Qin,  
21 G.-K. Plattner, M. Tignor, and P.M. Midgley (eds.)]. IPCC Working Group I Technical Support  
22 Unit, University of Bern, Bern, Switzerland.
- 23 Kuczera, G.: Combining site-specific and regional information: An empirical Bayes Approach,  
24 *Water Resour. Res.*, 18(2), 306–314, 1982.
- 25 Laaha, G. and Blöschl, G.: Seasonality indices for regionalizing low flows, *Hydrol. Process.*,  
26 20, 3851–3878, doi:10.1002/hyp.6161, 2006.
- 27 Laaha, G. and Blöschl, G.: A national low flow estimation procedure for Austria, *Hydrol. Sci.*  
28 *J.*, 52(4), 625–644, doi:10.1623/hysj.52.4.625, 2007.
- 29 Lins, H. F. and Slack, J. R.: Streamflow trends in the United States, *Geophys. Res. Lett.*, 26(2),  
30 227–230, 1999.
- 31 Loibl, W., Formayer, H., Schöner, W., Truhetz, H., Anders, I., Gobiet, A., Heinrich, G., Köstl,  
32 M., Nadeem, I., Peters-Anders, J. and others: Reclip: century 1 Research for climate protection:  
33 century climate simulations: models, data and ghg-scenarios, simulations, ACRP Final Rep.  
34 Reclip Century Part Vienna, 2011.
- 35 Lorenzo-Lacruz, J., Vicente-Serrano, S. M., López-Moreno, J. I., Morán-Tejeda, E. and  
36 Zabalza, J.: Recent trends in Iberian streamflows (1945–2005), *J. Hydrol.*, 414–415, 463–475,  
37 doi:10.1016/j.jhydrol.2011.11.023, 2012.
- 38 Luce, C. H., and Holden, Z. A.: Declining annual streamflow distributions in the Pacific  
39 Northwest United States, 1948-2006, *Geophys. Res. Lett.*, 36, L16401,  
40 doi:10.1029/2009GL039407, 2009.
- 41 Luce, C. H., Abatzoglou, J. T., and Holden, Z. A.: The Missing Mountain Water: Slower  
42 Westerlies Decrease Orographic Enhancement in the Pacific Northwest USA, *Science*, 342,  
43 1360-1364, DOI: 10.1126/science.1242335, 2013.

- 1 Majone, B., Bovolo, C. I., Bellin, A., Blenkinsop, S. and Fowler, H. J.: Modeling the impacts  
2 of future climate change on water resources for the Gállego river basin (Spain), *Water Resour.*  
3 *Res.*, 48(1), doi:10.1029/2011WR010985, 2012.
- 4 Merz, R. and Blöschl, G.: Flood frequency hydrology: 2. Combining data evidence, *Water*  
5 *Resour. Res.*, 44(8), doi:10.1029/2007WR006745, 2008.
- 6 Merz, R., Parajka, J. and Blöschl, G.: Time stability of catchment model parameters:  
7 Implications for climate impact analyses, *Water Resour. Res.*, 47(2), W02531,  
8 doi:10.1029/2010WR009505, 2011.
- 9 Montanari, A., Rosso, R., & Taqqu, M. S. (1997). Fractionally differenced ARIMA models  
10 applied to hydrologic time series: Identification, estimation, and simulation. *Water Resources*  
11 *Research*, 33(5), 1035-1044.
- 12 Parajka, J., Blaschke, A. P., Blöschl, G., Haslinger, K., Hepp, G., Laaha, G., Schöner, W.,  
13 Trautvetter, H., Viglione, A., and Zessner, M.: Uncertainty contributions to low-flow  
14 projections in Austria, *Hydrol. Earth Syst. Sci.*, 20, 2085-2101, doi:10.5194/hess-20-2085-  
15 2016, 2016.
- 16 Parajka, J., Merz, R. and Blöschl, G.: Uncertainty and multiple objective calibration in regional  
17 water balance modelling: case study in 320 Austrian catchments, *Hydrol. Process.*, 21(4), 435–  
18 446, doi:10.1002/hyp.6253, 2007.
- 19 Perdigão, R. A. P., and G. Blöschl (2014) Spatiotemporal flood sensitivity to annual  
20 precipitation: Evidence for landscape-climate coevolution, *Water Resour. Res.*, 50, 5492-5509,  
21 doi:10.1002/2014WR015365.
- 22 Prudhomme, C., Young, A., Watts, G., Haxton, T., Crooks, S., Williamson, J., Davies, H.,  
23 Dadson, S. and Allen, S.: The drying up of Britain? A national estimate of changes in seasonal  
24 river flows from 11 Regional Climate Model simulations, *Hydrol. Process.*, 26(7), 1115–1118,  
25 doi:10.1002/hyp.8434, 2012.
- 26 Prudhomme, C., Giuntoli, I., Robinson, E. L., Clark, D. B., Arnell, N. W., Dankers, R., Fekete,  
27 B. M., Franssen, W., Gerten, D., Gosling, S. N., Hagemann, S., Hannah, D. M., Kim, H.,  
28 Masaki, Y., Satoh, Y., Stacke, T., Wada, Y. and Wisser, D.: Hydrological droughts in the 21st  
29 century, hotspots and uncertainties from a global multimodel ensemble experiment, *Proc. Natl.*  
30 *Acad. Sci.*, doi:10.1073/pnas.1222473110, 2013.
- 31 Renard, B., Lang, M., Bois, P., Dupeyrat, A., Mestre, O., Niel, H., Sauquet, E., Prudhomme,  
32 C., Parey, S., Paquet, E., Neppel, L. and Gailhard, J.: Regional methods for trend detection:  
33 Assessing field significance and regional consistency, *Water Resour. Res.*, 44(8), W08419,  
34 doi:10.1029/2007WR006268, 2008.
- 35 Rodionov, S. N. (2006). Use of prewhitening in climate regime shift detection. *Geophysical*  
36 *Research Letters*, 33(12).
- 37 Samaniego, L., Kumar, R., & Zink, M. (2013). Implications of Parameter Uncertainty on Soil  
38 Moisture Drought Analysis in Germany. *Journal of Hydrometeorology*, 14(1), 47–68.  
39 <http://doi.org/10.1175/JHM-D-12-075.1>
- 40 Schöner, W., Böhm, R. and Auer, I.: 125 years of high-mountain research at Sonnblick  
41 Observatory (Austrian Alps)—from “the house above the clouds” to a unique research platform,  
42 *Theor. Appl. Climatol.*, 110(4), 491–498, 2012.
- 43 Sen, P. K. (1968). Estimates of the regression coefficient based on Kendall's tau. *Journal of the*  
44 *American Statistical Association*, 63(324), 1379-1389.

- 1 Sheffield, J., Wood, E. F. and Roderick, M. L.: Little change in global drought over the past 60  
2 years, *Nature*, 491(7424), 435–438, 2012.
- 3 Sivapalan, M., Blöschl, G., Zhang, L. and Vertessy, R.: Downward approach to hydrological  
4 prediction, *Hydrol. Process.*, 17(11), 2101–2111, doi:10.1002/hyp.1425, 2003.
- 5 Sivapalan, M., Blöschl, G., Merz, R. and Gutknecht, D.: Linking flood frequency to long-term  
6 water balance: Incorporating effects of seasonality, *Water Resour. Res.*, 41(6),  
7 doi:10.1029/2004WR003439, 2005.
- 8 Stahl, K., Hisdal, H., Hannaford, J., Tallaksen, L. M., van Lanen, H. A. J., Sauquet, E., Demuth,  
9 S., Fendekova, M. and Jódar, J.: Streamflow trends in Europe: evidence from a dataset of near-  
10 natural catchments, *Hydrol. Earth Syst. Sci.*, 14(12), 2367–2382, doi:10.5194/hess-14-2367-  
11 2010, 2010.
- 12 Stedinger, J. R. and Tasker, G. D.: Regional hydrologic analysis: 1. Ordinary, weighted, and  
13 generalized least squares compared, *Water Resour. Res.*, 21(9), 1421–1432, 1985.
- 14 Szolgayová, E., Laaha, G., Blöschl, G. and Bucher, C.: Factors influencing long range  
15 dependence in streamflow of European rivers, *Hydrol. Process.*, 28(4), 1573–1586, 2014.
- 16 Thyer, M. and Kuczera, G.: A hidden Markov model for modelling long-term persistence in  
17 multi-site rainfall time series 1. Model calibration using a Bayesian approach, *J. Hydrol.*,  
18 275(1), 12–26, 2003.
- 19 Van Loon, A. F. and Laaha, G.: Hydrological drought severity explained by climate and  
20 catchment characteristics, *J. Hydrol.*, 526, 3–14, doi:10.1016/j.jhydrol.2014.10.059, 2015.
- 21 Vicente-Serrano, S. M., Beguería, S. and López-Moreno, J. I.: A multiscalar drought index  
22 sensitive to global warming: the standardized precipitation evapotranspiration index, *J. Clim.*,  
23 23(7), 1696–1718, 2010.
- 24 Viglione, A. and Parajka, J.: TUWmodel: Lumped Hydrological Model for Education Purposes.  
25 R package. [online] Available from: <http://CRAN.R-project.org/package=TUWmodel>, 2014.
- 26 Viglione, A., Castellarin, A., Rogger, M., Merz, R. and Blöschl, G.: Extreme rainstorms:  
27 Comparing regional envelope curves to stochastically generated events, *Water Resour. Res.*,  
28 48(1), doi:10.1029/2011WR010515, 2012.
- 29 Viglione, A., Merz, R., Salinas, J. L. and Blöschl, G.: Flood frequency hydrology: 3. A  
30 Bayesian analysis, *Water Resour. Res.*, 49(2), 675–692, doi:10.1029/2011WR010782, 2013.
- 31 Watts, G., von Christierson, B., Hannaford, J. and Lonsdale, K.: Testing the resilience of water  
32 supply systems to long droughts, *J. Hydrol.*, 414, 255–267, 2012.
- 33 Wilby, R. L. and Dessai, S.: Robust adaptation to climate change, *Weather*, 65(7), 180–185,  
34 2010.
- 35 Wilson, E. O.: *Consilience: the unity of knowledge*. New York: Knopf, 1998.
- 36 Wilson, D., Hisdal, H. and Lawrence, D.: Has streamflow changed in the Nordic countries? –  
37 Recent trends and comparisons to hydrological projections, *J. Hydrol.*, 394(3-4), 334–346,  
38 doi:10.1016/j.jhydrol.2010.09.010, 2010.
- 39 Winsemius, H. C., Schaefli, B., Montanari, A. and Savenije, H. H. G.: On the calibration of  
40 hydrological models in ungauged basins: A framework for integrating hard and soft  
41 hydrological information, *Water Resour. Res.*, 45(12) [online] Available from:

1 <http://onlinelibrary.wiley.com/doi/10.1029/2009WR007706/full> (Accessed 3 November  
2 2015), 2009.

3 Wong, W. K., Beldring, S., Engen-Skaugen, T., Haddeland, I. and Hisdal, H.: Climate Change  
4 Effects on Spatiotemporal Patterns of Hydroclimatological Summer Droughts in Norway, *J.*  
5 *Hydrometeorol.*, 12(6), 1205–1220, doi:10.1175/2011JHM1357.1, 2011.

6 Yue, S., Pilon, P., Phinney, B. and Cavadias, G.: The influence of autocorrelation on the ability  
7 to detect trend in hydrological series, *Hydrol. Process.*, 16(9), 1807–1829, 2002.

8

9

1

2 Table 1. Trend estimates of observed Q<sub>95</sub> low flows in the period 1976-2008 (Mann-Kendall  
3 test). Relative trends refer to the trend over the observation period relative to its mean.

	Hoalp	Muhl	Gurk	Buwe
Trend (m <sup>3</sup> /s per 100 yrs)	+0.24 **	-0.28	-1.45	-0.34 *
Relative trend (% per year)	+1.21 **	-0.38	-0.78	-1.88 *
p-value	0.009	0.377	0.053	0.045

4 Significance codes: \*\* p<0.01 ; \* p< 0.05

5

6

1 Table 2. Trend extrapolations of average  $Q_{95}$  low flows ( $m^3/s$ ) for the periods 2021-2050 and  
 2 2051-2080 based on observed trends. Changes (%) refer to the  $Q_{95}$  in the future period relative  
 3 to the average  $Q_{95}$  in the reference period (1976-2008). Values in parentheses indicate 95%  
 4 confidence intervals.

		Hoalp	Muhlv	Gurk	Buwe
2021-2050	$Q_{95}$ ( $m^3/s$ )	0.28 (0.19, 0.37)	0.68 (0.45, 1.02)	1.19 (0.58, 2.00)	0.02 (-0.14, 0.14)
2021-2050	Change (%)	+39 (-7, +71)	-8 (-41, +34)	-36 (-72, -1)	-90 (-177, -22)
2051-2080	$Q_{95}$ ( $m^3/s$ )	0.35 (0.22, 0.45)	0.60 (0.15, 1.14)	0.74 (-0.23, 2.01)	-0.08(-0.33, 0.12)
2051-2080	Change (%)	+74 (0, 123)	-21 (-79, +51)	-59 (-113, +9)	-148 (-282, -36)

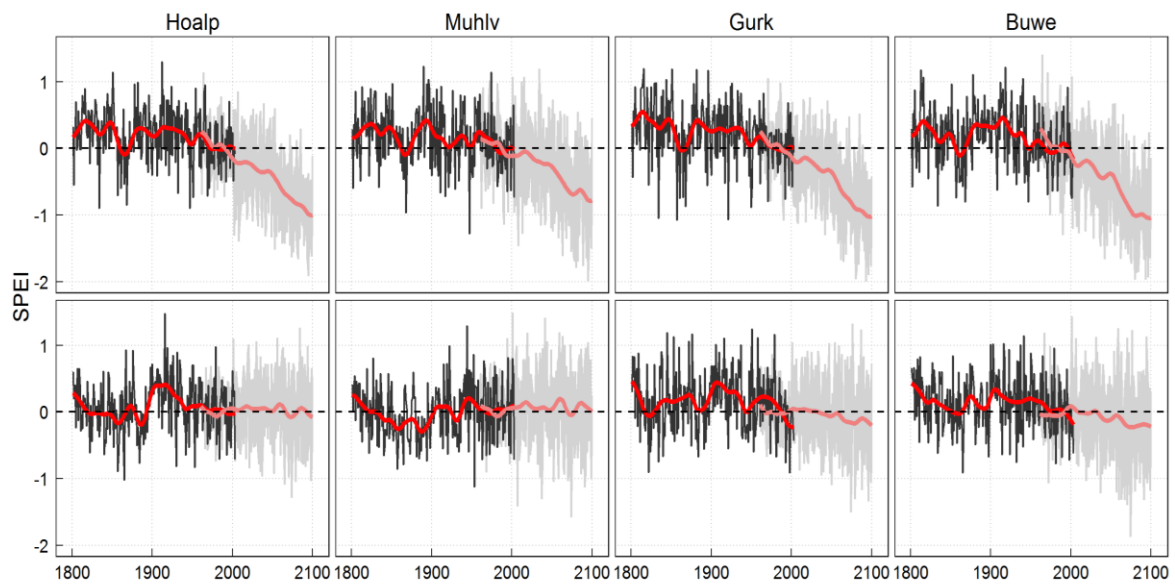
5

6

1 Table 3. Runoff model efficiency  $Z_Q$  (Eq. 2) obtained for different weights  $w_Q$  in the four  
 2 catchments for three calibration periods.  $w_Q = 0$  and  $w_Q = 1$  emphasise low flows and high flow,  
 3 respectively, in the calibration.  $Z_Q$  are listed in the sequence of the calibration periods: 1976-  
 4 1986/1987-1997/1998-2008.

$w_Q$	Hoalp	Muhlv	Gurk	Buwe
0.0	0.96/0.95/0.90	0.82/0.84/0.86	0.79/0.73/0.79	0.46/0.52/0.59
0.1	0.95/0.93/0.90	0.81/0.83/0.86	0.79/0.73/0.79	0.37/0.52/0.58
0.2	0.94/0.92/0.90	0.80/0.82/0.86	0.78/0.74/0.79	0.35/0.53/0.58
0.3	0.93/0.90/0.90	0.79/0.81/0.86	0.78/0.74/0.79	0.34/0.54/0.58
0.4	0.92/0.89/0.89	0.79/0.80/0.86	0.78/0.74/0.79	0.40/0.54/0.57
0.5	0.91/0.88/0.89	0.77/0.79/0.86	0.78/0.75/0.78	0.36/0.55/0.56
0.6	0.90/0.86/0.89	0.77/0.78/0.86	0.78/0.75/0.78	0.30/0.56/0.55
0.7	0.89/0.85/0.89	0.76/0.78/0.86	0.78/0.75/0.78	0.30/0.57/0.55
0.8	0.88/0.83/0.75	0.76/0.77/0.81	0.78/0.76/0.80	0.30/0.58/0.49
0.9	0.88/0.82/0.73	0.75/0.76/0.81	0.78/0.76/0.80	0.28/0.59/0.49
1.0	0.87/0.82/0.72	0.75/0.75/0.81	0.78/0.77/0.81	0.29/0.60/0.49

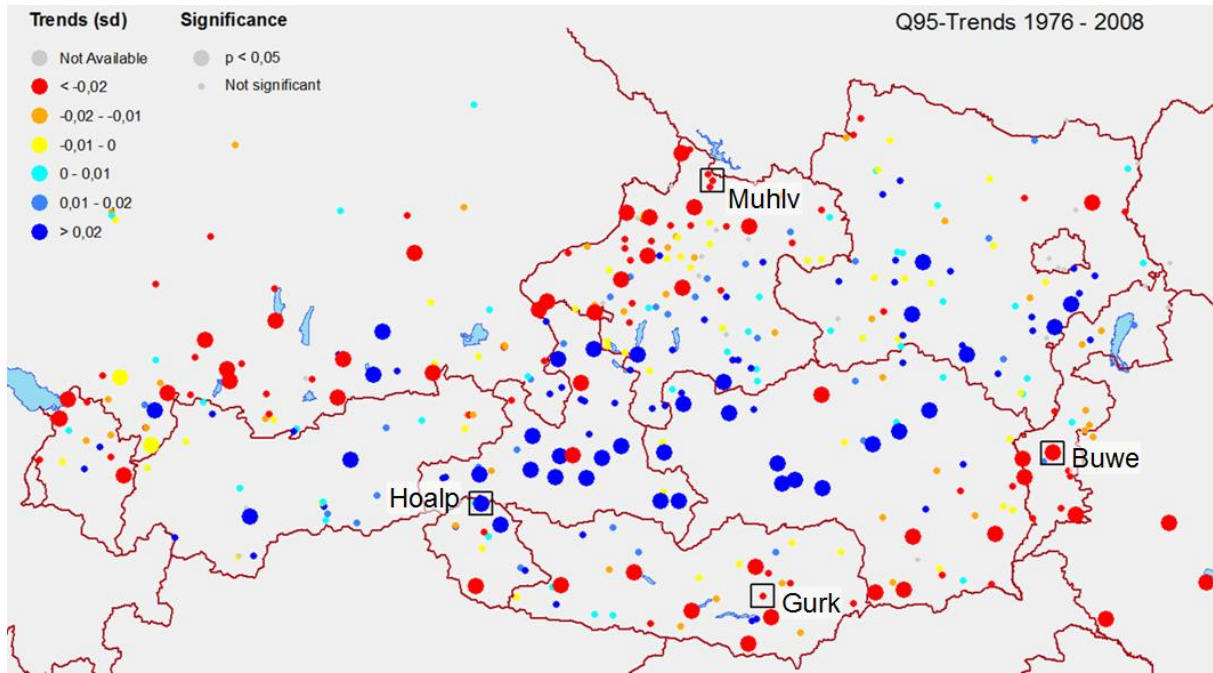
5  
6



1  
 2 Figure 1. Standardized precipitation evaporation index (SPEI) in summer (top) and winter  
 3 (bottom) (three month averages of monthly values) for the four example catchments. Observed  
 4 (HISTALP, Auer et al., 2007, black) and projected (reclip:century ensemble spread, grey). Red  
 5 and light red lines represent the Gaussian low-pass filtered values of the observed and projected  
 6 SPEI, respectively.

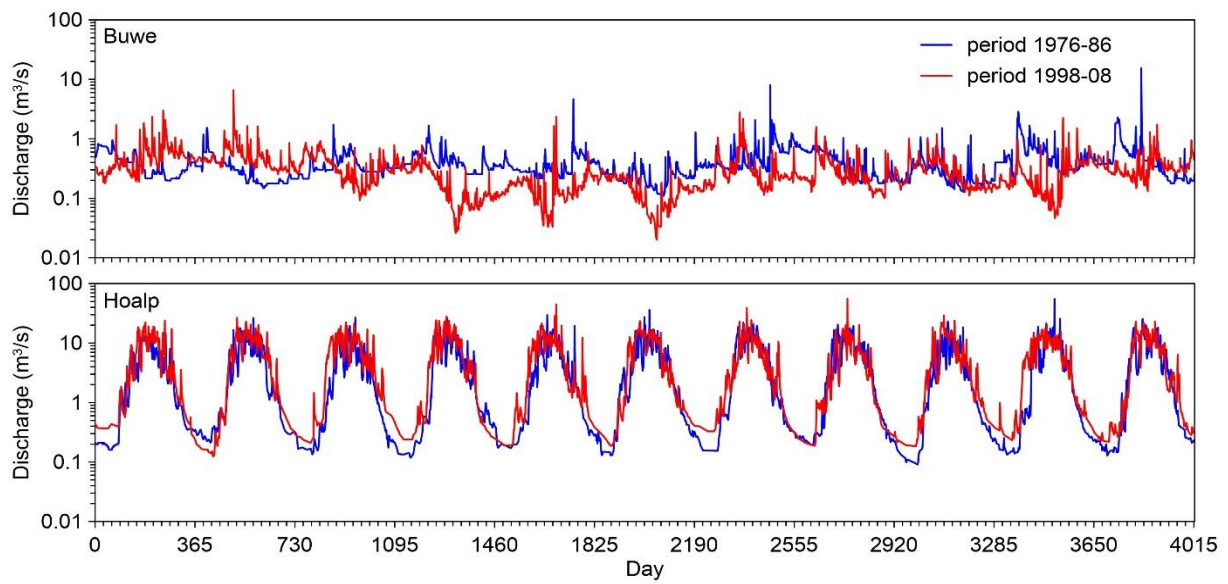


1

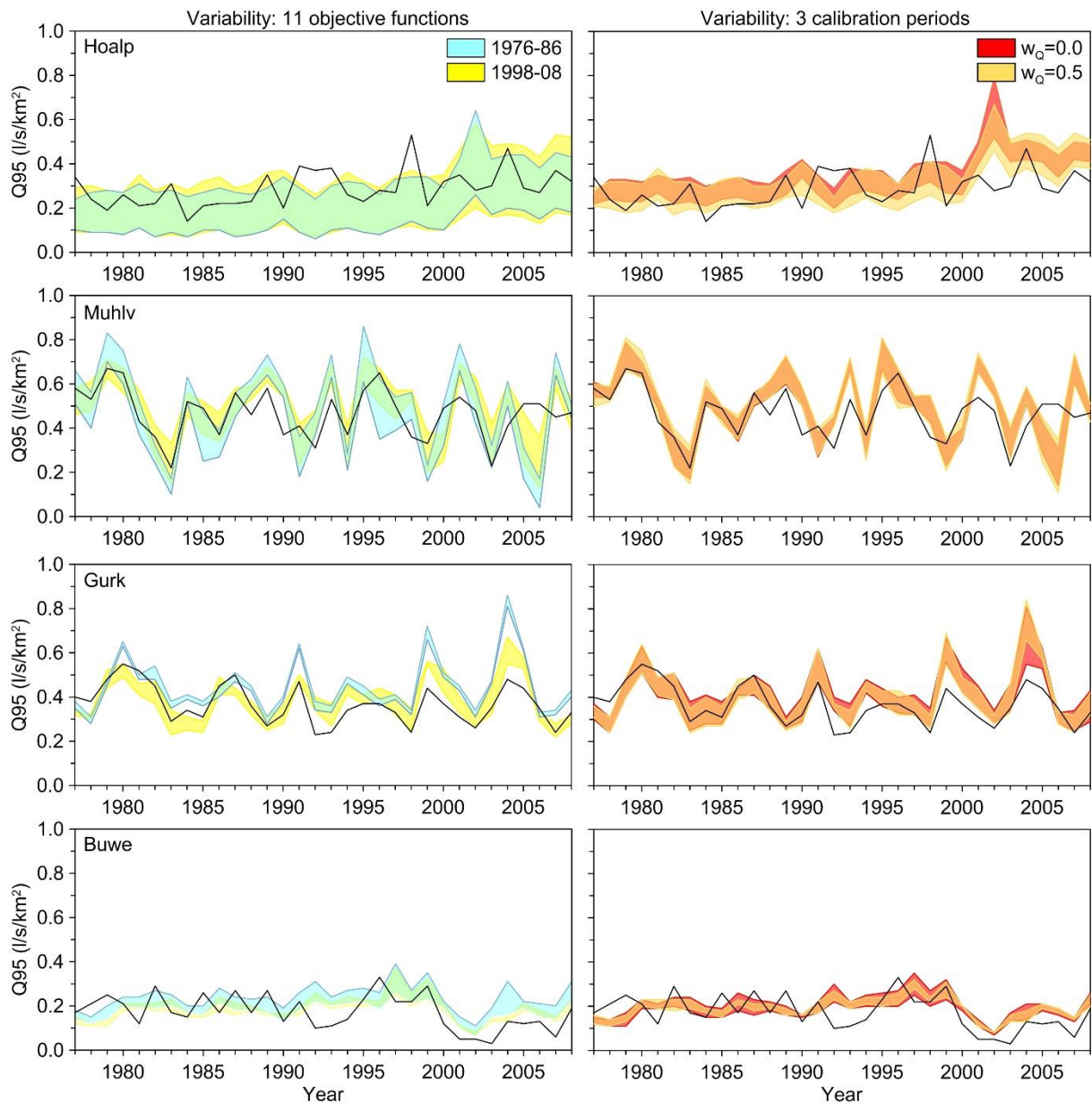


2

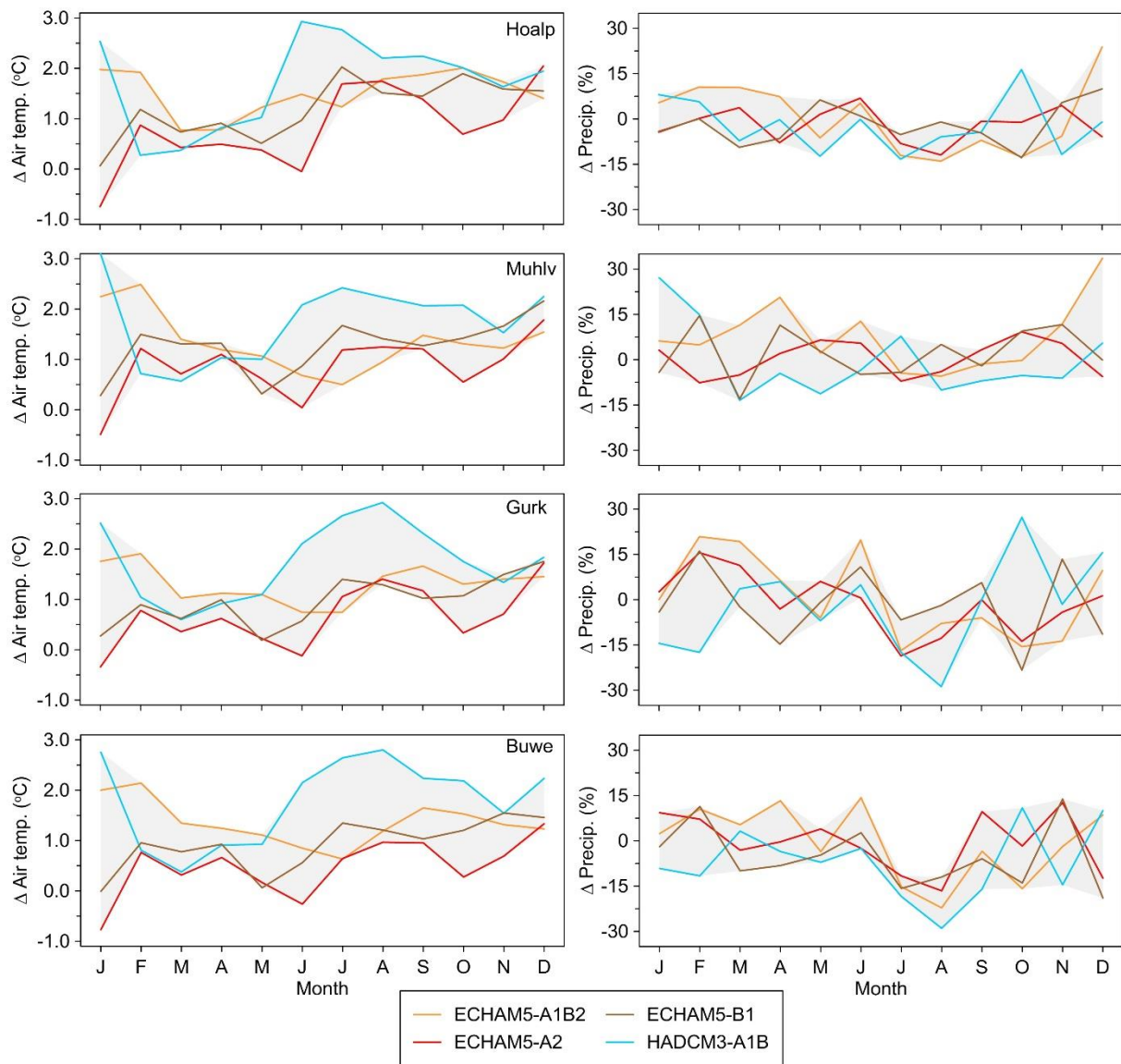
3 Figure 2. Observed trends of annual  $Q_{95}$  low flows in Austria in the period 1976-2008. Colours  
4 correspond to the sign and the magnitude of the trends (blue = increasing, red = decreasing).  
5 Size indicates significance of trends. Units of the trends are standard deviations per year.  
6 Squares indicate example catchments.



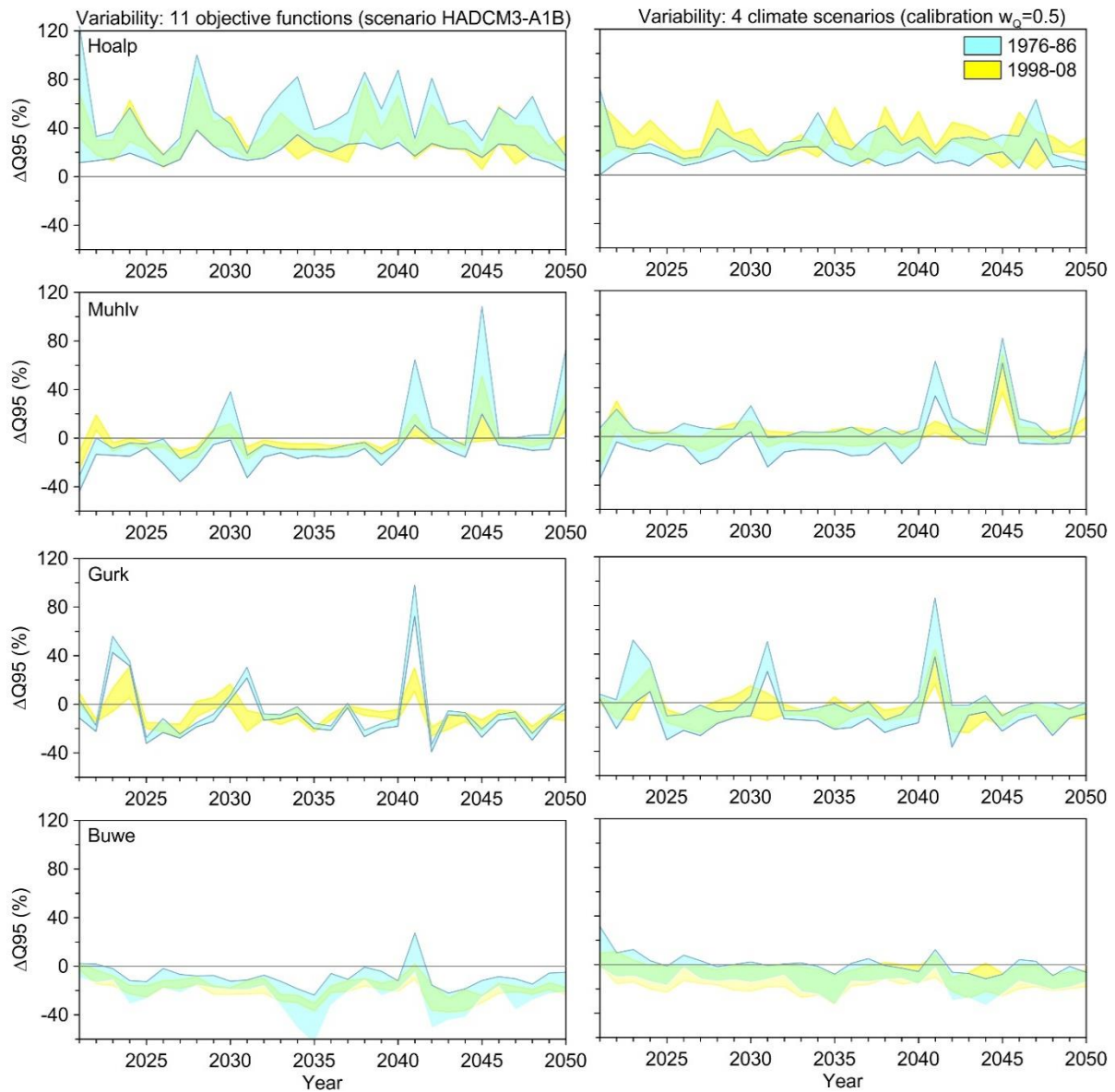
1  
2 Figure 3: Observed daily discharge for the periods 1976-1986 (blue lines) and 1998-2008 (red  
3 lines) in the Buwe (top) and Hoalp (bottom) catchments.



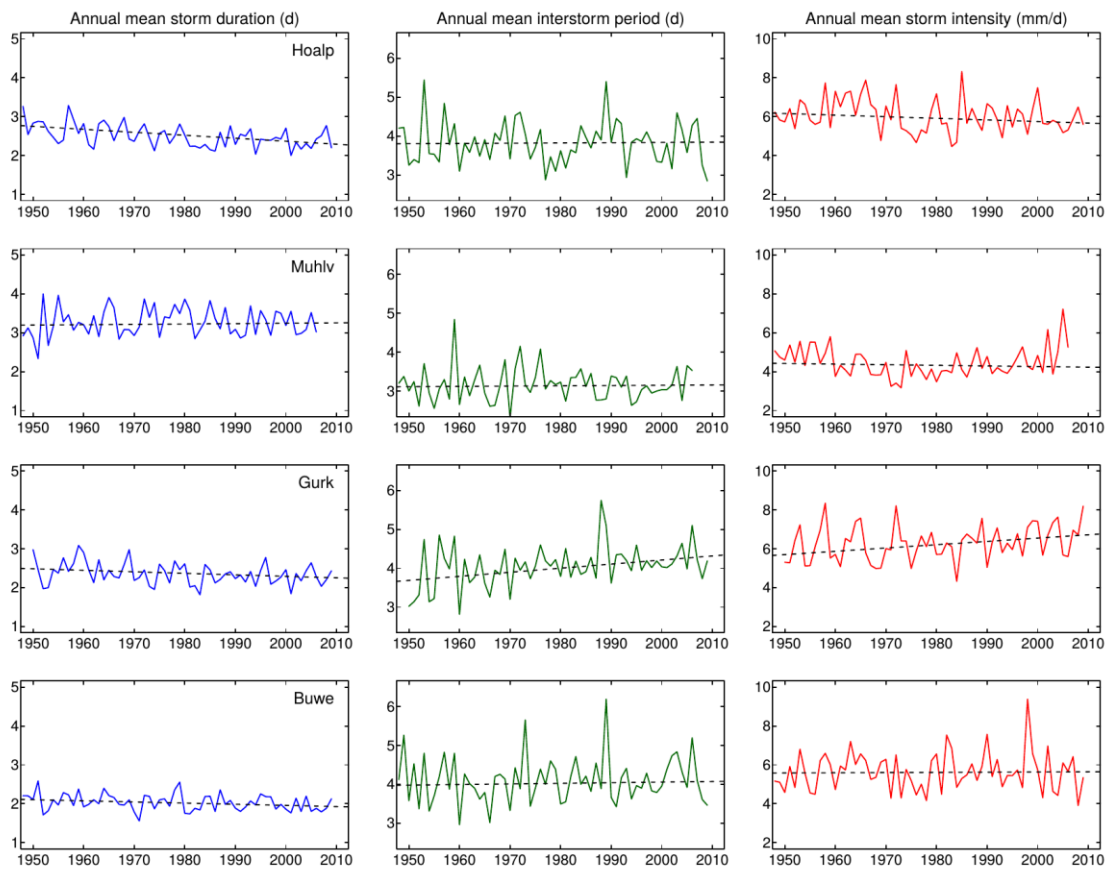
1  
 2 Figure 4. Annual  $Q_{95}$  low flows from observed data (black lines) and from hydrologic model  
 3 simulations (coloured bands) for the four catchments. Band widths in the left panels show the  
 4 variability due to different weights  $w_Q$  in the objective function (Table 3) for two calibration  
 5 periods (1976-1986 and 1998-2008). Band widths in the right panels show the variability due  
 6 to different decades used for model calibration for two sets of weights ( $w_Q=0.5$  and  $w_Q=0.0$ ).



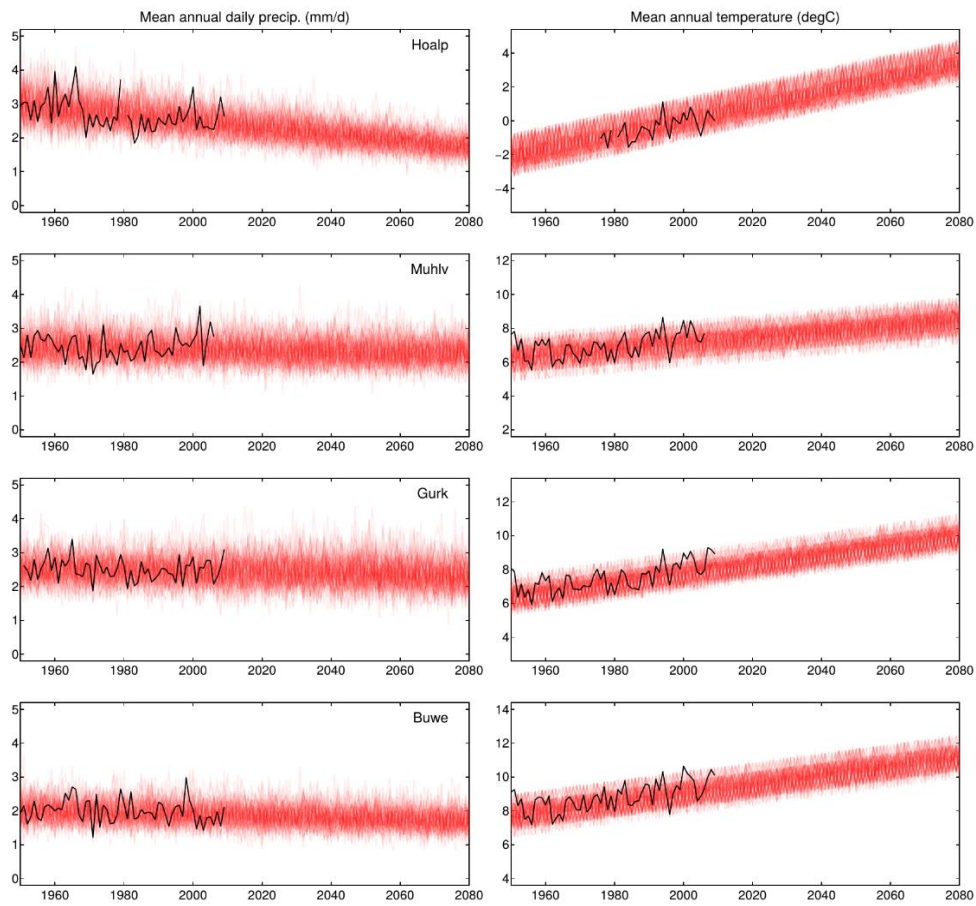
1  
 2 Figure 5. Projections of air temperatures and precipitation for the four catchments simulated by  
 3 regional climate models. Shown are long-term monthly changes of the future period (2021-  
 4 2050) relative to the reference period (1976-2008). Shaded areas indicate the range of climate  
 5 scenarios/models.



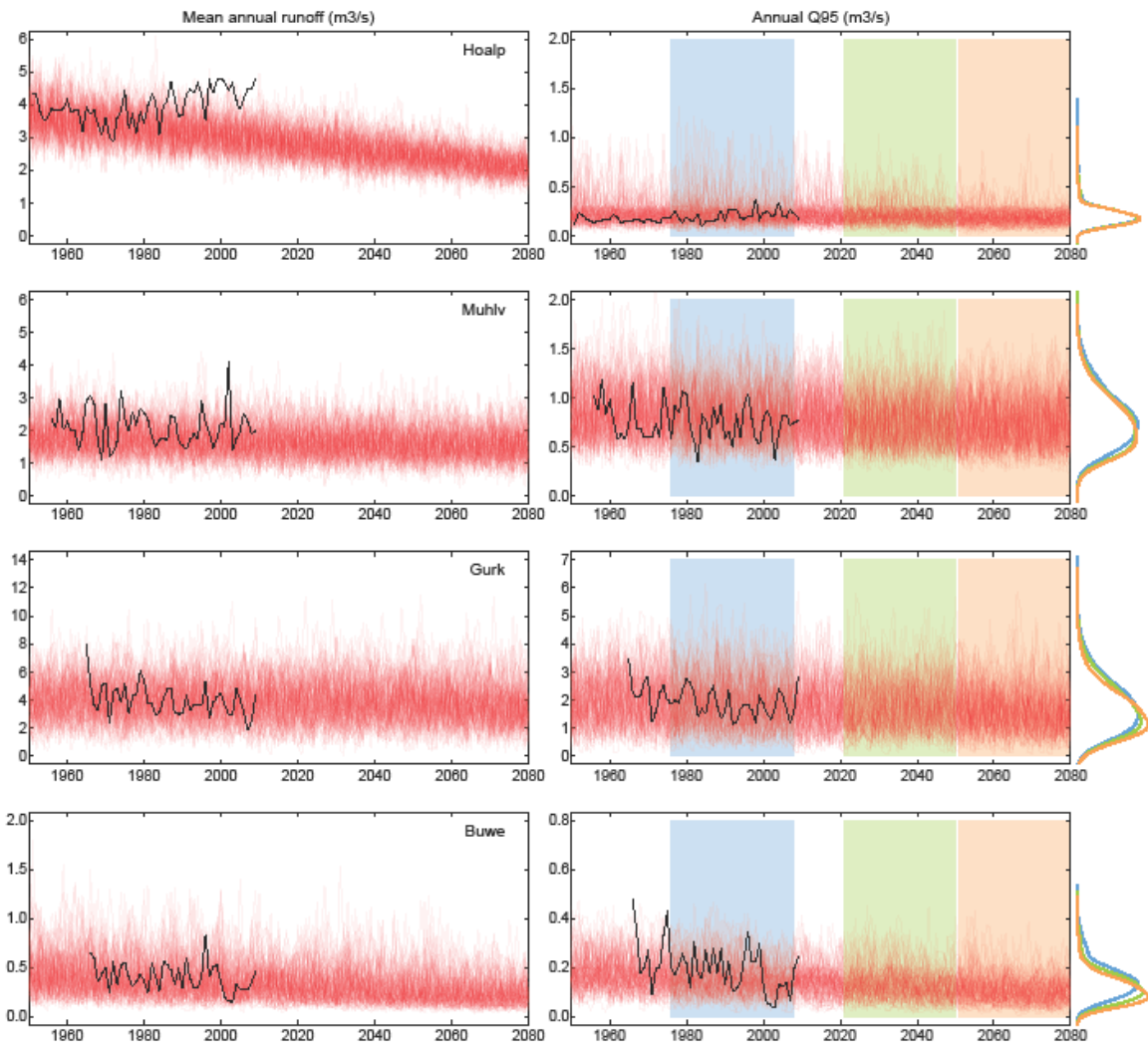
1  
2 Figure 6. Projections of annual  $Q_{95}$  low flows for the four catchments in terms of changes of  
3 the future period (2021-2050) relative to simulated runoff in the reference period (1976-2008).  
4 Band widths in the left panels show the variability due to different weights  $w_Q$  in the objective  
5 function (Table 3) using HADCM3. Band widths in the right panels show the variability due to  
6 the choice of climate projections for calibration variant  $w_Q=0.5$ . Yellow and blue colours relate  
7 to two calibration periods for the hydrological model.



1  
 2 Figure 7. Observed trends in the precipitation statistics for the climate stations St. Jakob Def  
 3 (Hoalp), Pabneukirchen (Muhlv), Klagenfurt (Gurk) and Woerterberg (Buwe). The trend lines  
 4 (dashed) have been fitted with the Theil-Sen method.

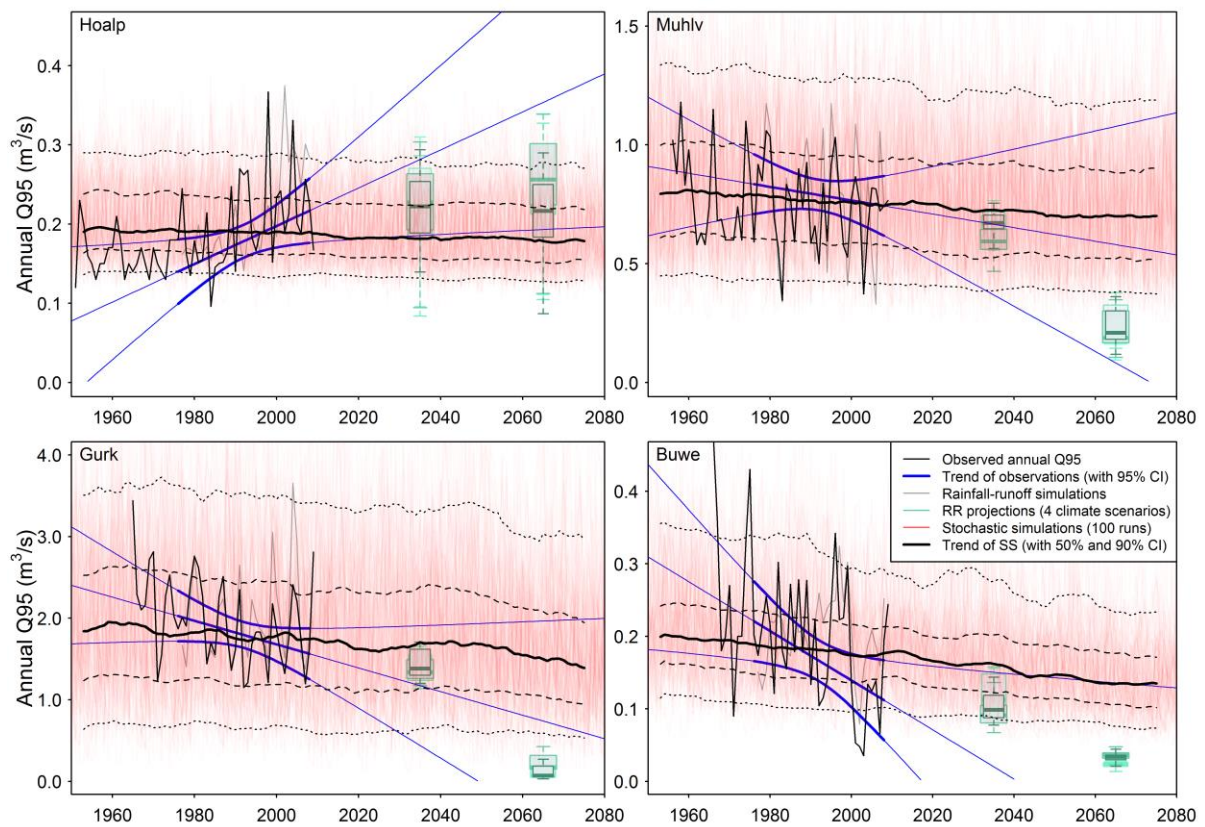


1  
 2 Figure 8. Stochastic simulations of mean annual precipitation and mean annual temperature  
 3 (red lines) for St. Jakob Def (Hoalp), Pabneukirchen (Muhlv), Klagenfurt (Gurk) and  
 4 Woerterberg (Buwe). 100 simulated time series for each station. For comparison, observations  
 5 are shown (black lines).

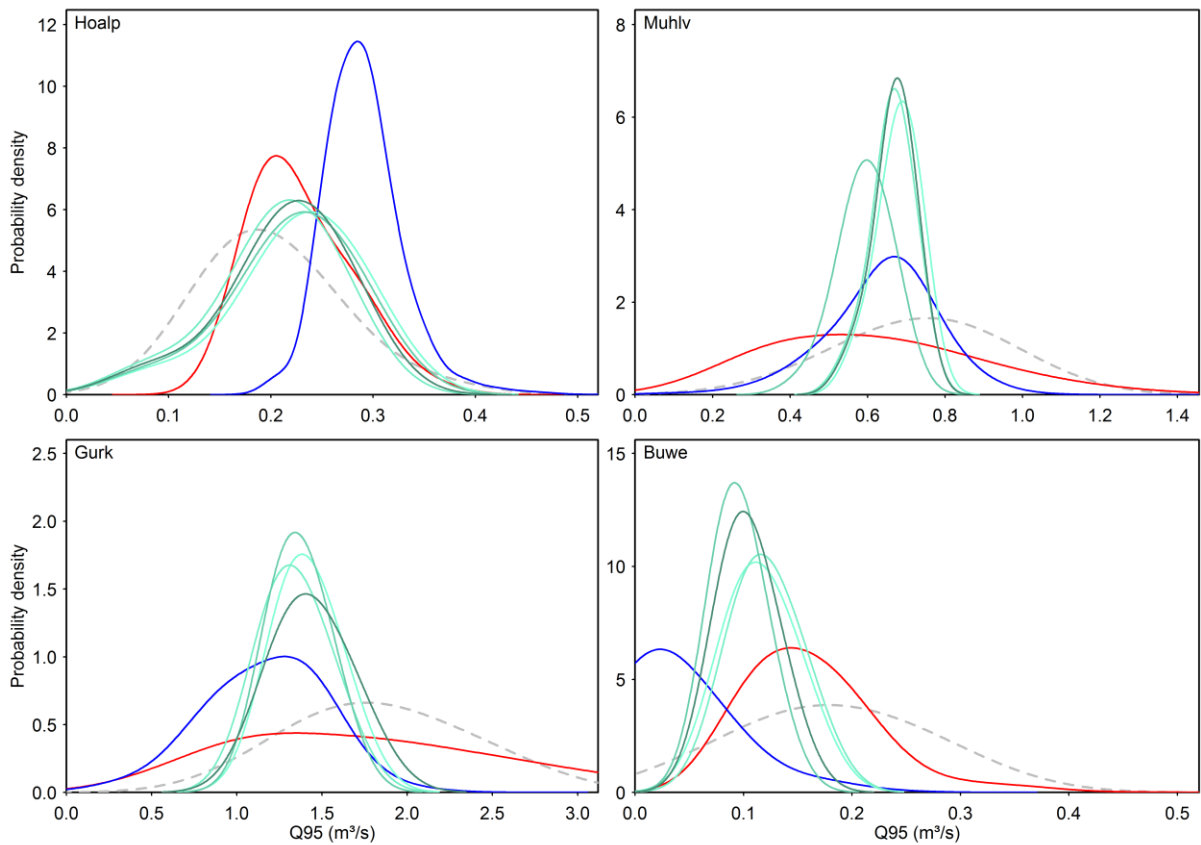


1  
 2 Figure 9. Stochastic simulations of mean annual runoff and annual  $Q_{95}$  (red lines) assuming  
 3 linear extrapolation of the rainfall model parameters for the Hoalp, Muhlv, Gurk and Buwe  
 4 catchments. 100 simulated time series for each catchment. For comparison, observations are  
 5 shown (black lines). Probability density functions of  $Q_{95}$  for three periods are shown on the  
 6 right.





1  
 2 Figure 10. Three-pillar projections of annual  $Q_{95}$  low flows for the Hoalp, Muhlv, Gurk and  
 3 Buwe catchments. Black lines refer to observed annual  $Q_{95}$ . Pillar 1: extrapolation of observed  
 4 low flow trends (blue) and 0.95 level confidence bounds (blue curved lines); bold/thin parts  
 5 refer to observation/extrapolation period. Pillar 2: simulations in the observation period (gray  
 6 line), and climate projections and runoff modelling for 2021-2050 and 2051-2080 (box plots,  
 7 shades of green indicate different climate scenarios, range of box plots indicates different  
 8 parameters of the hydrological model). Pillar 3: extrapolation of stochastic rainfall  
 9 characteristics and runoff modelling (100 realisations, red lines) with 0.50 level (black dashed  
 10 lines) and 0.90 level (black dotted lines) confidence bounds.



1  
 2 Figure 11. Probability density functions (pdf) of annual Q<sub>95</sub> low flows 2021-2050 of the three-  
 3 pillar projections for the Hoalp, Muhlv, Gurk and Buwe catchments as in Figure 10. Pillar 1:  
 4 extrapolation of observed low flows (blue). Pillar 2: climate projections and runoff modelling  
 5 (different shades of green) Pillar 3: Extrapolation of stochastic rainfall characteristics and runoff  
 6 modelling (red). The pdfs represent both variability within the period and uncertainty (pillars 1  
 7 and 2) and variability alone (pillar 3). For comparison, observed Q<sub>95</sub> in the reference period  
 8 (1976-2008) is shown (dashed grey line).